CHAPTER 4

RESULTS AND

DISCUSSION

4.1 Synthesis of MgCuZn Ferrites by Co-precipitation Process

4.1.1 The Investigation of MgCuZn Ferrites By Co-precipitation Process

In recent years, the trend of electronics has been for an increasingly compact design. Electronic equipment is becoming smaller in size, lighter, multi functional and high performance. Miniaturization technology has been essential for making portable products such as video cameras, notebook computers, hard disk drives, cellular phones, portable radios and etc. Magnetic materials especially ferrites have been used in many applications and can be prepared using co-precipitation method.

In the past, nickel ferrites [57], magnesium ferrites [59] and zinc ferrites [60] that have been prepared by co-precipitation show a better magnetic behaviour than the ones prepared by conventional ceramics method. Therefore, MgCuZn ferrites have been prepared by co-precipitation process and the formation of ferrites has been determined qualitatively to identify the spinel phase formation and the surface morphology.

ICP analysis

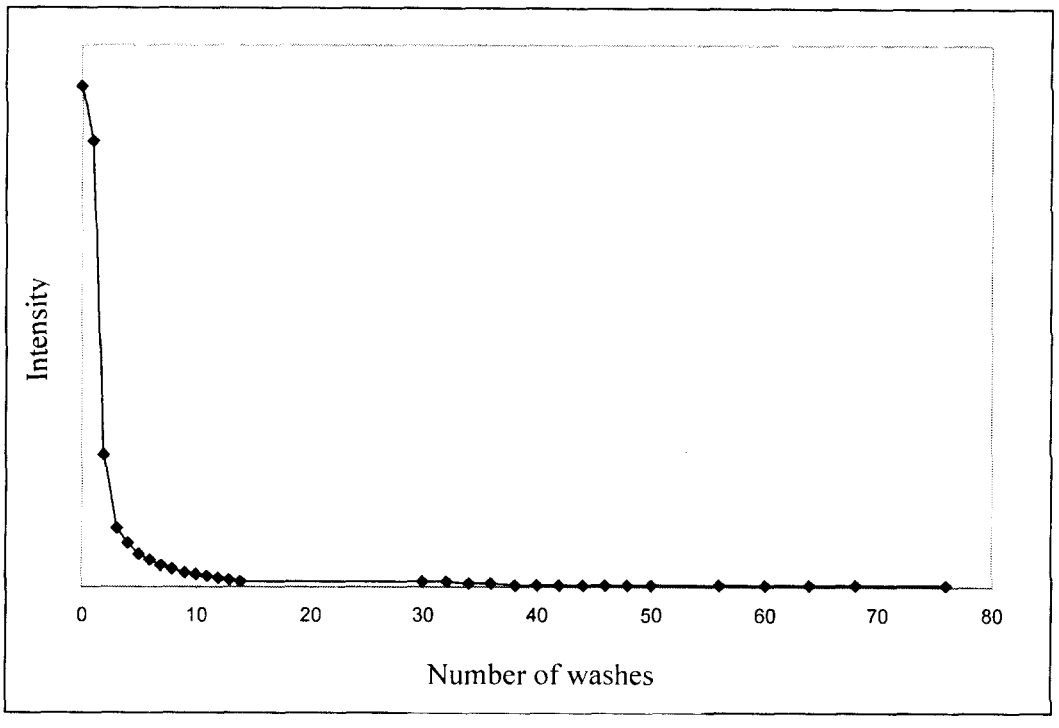

Fig. 4.1.1: ICP analysis for Na^+ ions determination before calcination

After all the starting materials have been mixed and formed the precipitate, the precipitate was washed with deionised water for different batches according to different number of washes for ICP testing. The ICP analysis (Fig. 4.1.1) is done to study the effectiveness of washing with deionised water. ICP analysis shows that about 40 washes or using 1000 ml deionised water, the concentration of Na^+ ions can be reduced to the minimum level. Therefore, in this study, the precipitate will be washed 40 times (1000ml deionised water) before calcination takes place. The precipitate was dark–brown in colour.

Thermal analysis

After 40 washes and dry, 20.4mg of precursor was subjected to TGA and SDTA analysis. TGA analysis (Fig. 4.1.2) reveals that the precipitate continuously loses weight from room temperature to about 400°C. The amount of weight lose is about 1.5 mg. Then, a small loss in weight is observed from 400°C to about 650°C.

SDTA analysis (Fig. 4.1.3) reveals that decomposition takes place from room temperature to about 180°C. Then, high rate of decomposition was observed from 180°C to about 400°C. After that, low rate of decomposition continuously occurs.

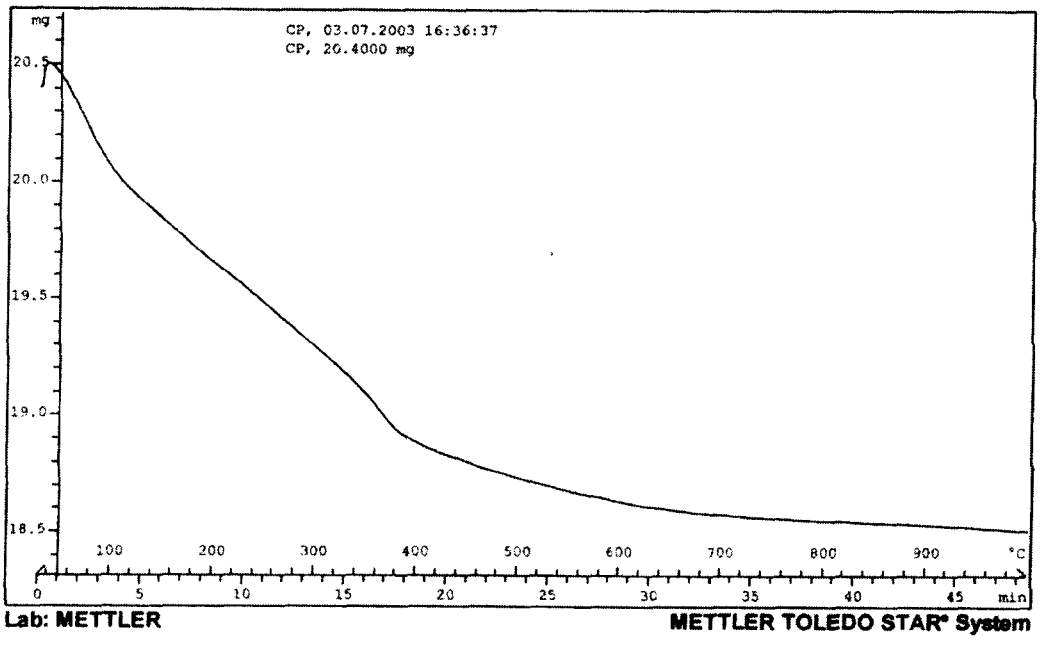

Fig. 4.1.2: TGA analysis for co-precipitated specimens after 40 washes

From the TGA and SDTA curves, it can be observed that dehydration happens at about 180°C, while ferritization (formation of ferrite) was started around 400°C. Although ferritization takes place at a temperature of around 400°C, in order to improve the crystallinity or to obtain the spinel structure, the precursor was further calcined at a temperature of 650°C.

Therefore, the precursor needs to be calcined in two stages. Two stage calcination is required to minimize segregation of component oxides (especially ZnO), which would happen as a result of overheating during the oxidation process, and to reduce the potential of loss in ZnO by volatilisation. In stage 1, the precursor will be heated at 400°C for 2 hours followed by stage 2, in which the calcination takes place at a temperature of 650°C for 2 hours.

Over calcination needs to be avoided as this will pre – sinter the ferrite powders and agglomerates and larger particles of ferrite may be formed. Consequently, it will affect the microstructure and electromagnetic properties of the final product.

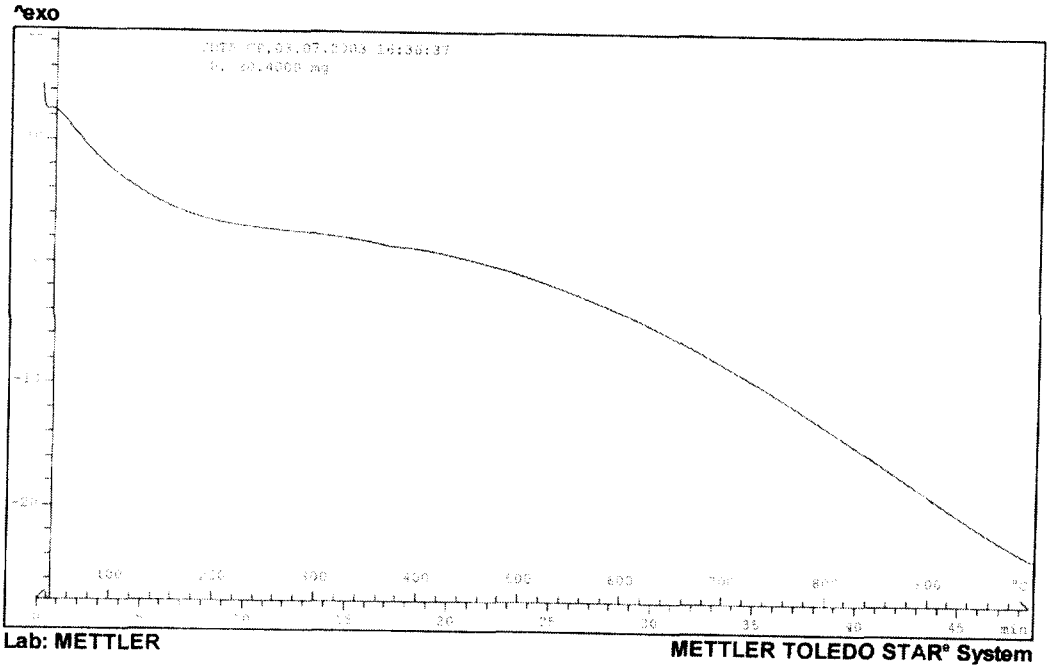

Fig. 4.1.3: SDTA analysis for co-precipitated specimens after 40 washes

XRD analysis

The XRD patterns of co-precipitated MgCuZn ferrite system are shown in Fig. 4.1.4. For powder without washing (no. 1), the XRD pattern shows that NaCl matches to the peaks and there is no sign of ferrite formation. After washing 40 times (no. 2), the

XRD shows that the powder is amorphous in nature because no clear diffraction peaks of crystalline phases were observed. According to Huang and Egon [57], in the co-precipitation process the individual metal hydroxides may form first after the precipitated powder is washed, which then react with each other to yield spinel ferrites, according to

$$x\,M(OH)_2 + (1-x)\,Fe(OH)_2 + 2\,Fe(OH)_3$$

$$\Leftrightarrow M_x Fe_{3-x} O_4 + 4H_2O \quad \text{(4.1.1)}$$

Where, $0 \leq x \leq 1$ and M is a divalent metal. Therefore, the precipitate in the amorphous phase can be expected to be metal hydroxide.

According to Fig. 4.1.3, dehydration occurred at a temperature of about 180°C and this result is confirmed by XRD analysis (Fig 4.1.4, no. 3) and Fig. 4.1.5, where the ferrite powder after drying at 180°C shows ferritization has occurred. The XRD patterns match well with the characteristic reflections of $MgFe_2O_4$ with no unidentified extra peak and were identified as single spinel phase. This can be explained from equation (4.1.1), where the spinel phase and water or vapour is formed. The water can be removed by dehydration. Therefore, it shows that partial ferritization has occurred at the dehydration temperature of 180°C.

However, further calcination is required to improve the crystallinity of ferrites. XRD analysis shows that semi-crystalline material is formed when the powder is heated to 400°C (no. 4). In order to further increase the crystallinity, powder is required to be further calcined at 650°C. The XRD peak of sample no. 5 (Fig. 4.1.4) shows that diffraction peak broadening is slightly decreased and the diffraction peak has sharpened as compared to the powders dried at 180°C and heated at 400°C. The sharpness of the major peaks and diffraction line narrowing of powder calcined at 650°C is probably due to a better order structure. [24]

For the compacted pellet sintered at 950°C (Fig. 4.1.4, no. 6) and Fig. 4.1.6, the XRD diagram shows that complete formation of a single phase spinel structure has occurred, resulting in high sharpness of the peaks and highly narrowing of the diffraction line. According to Shi et al. [61], the narrowing of the diffraction line and high sharpness is due to the better order structure or the increase of grain size.

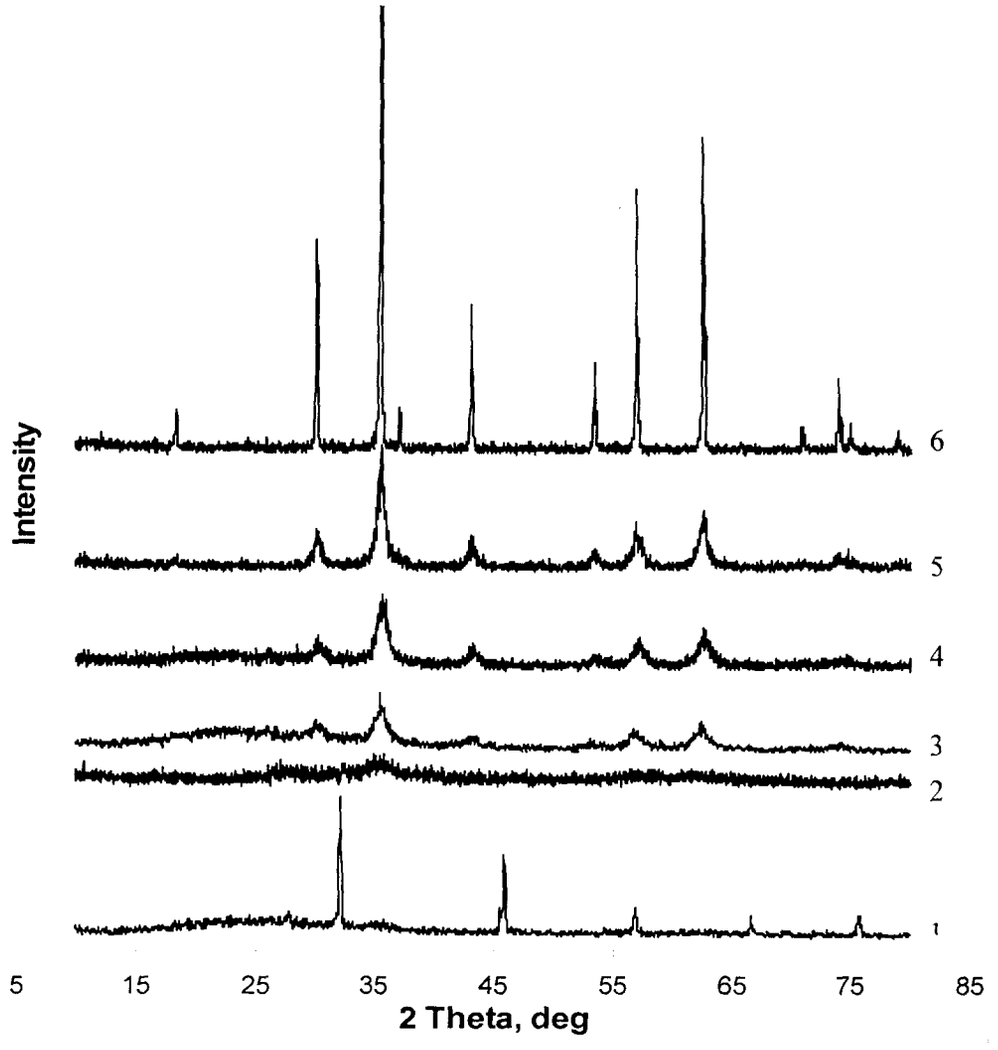

Fig. 4.1.4: XRD analysis for co-precipitated specimens, powder without washing (no. 1), after washing (no. 2), powder dried at 180°C (no. 3), powder heated at 400°C (no. 4), powder calcined at 650°C (no. 5) and pellet sintered at 950°C (no. 6)

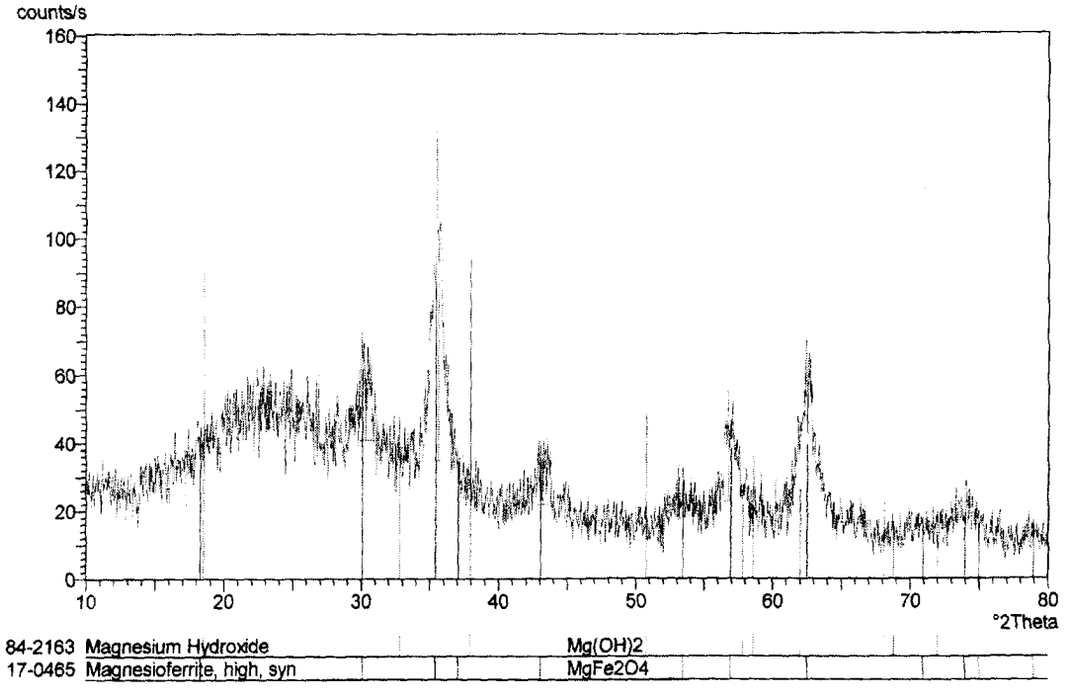

Fig. 4.1.5: XRD analysis of dehydrated powder at 180°C

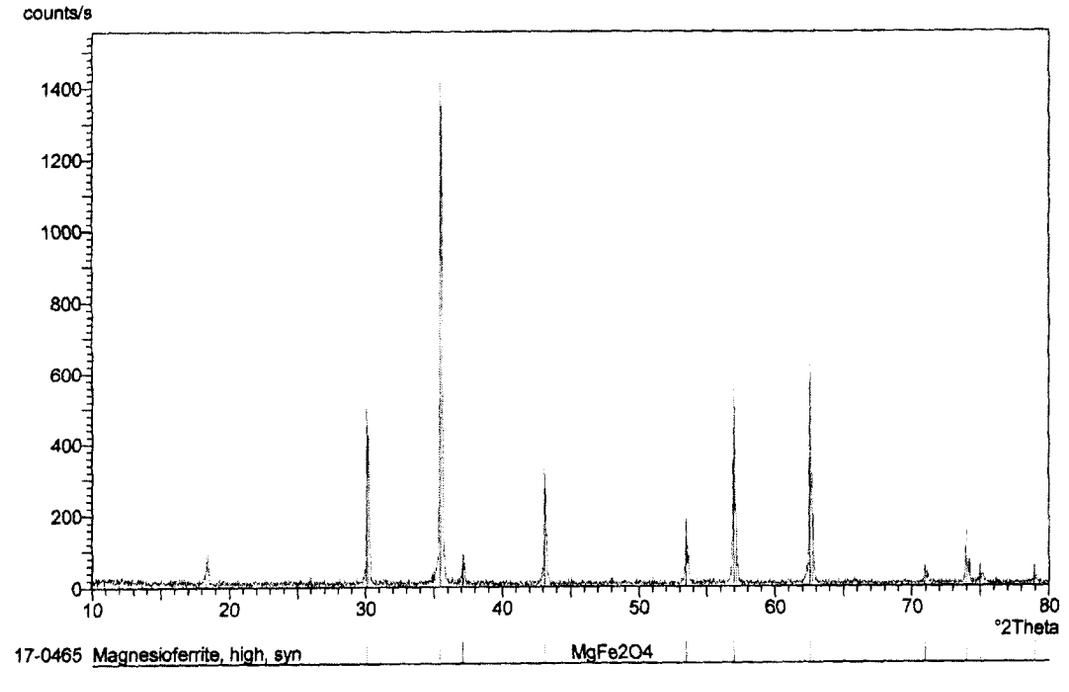

Fig. 4.1.6: XRD analysis for pellet sinter at 950°C

Overall, the intensity (counts/second) of the diffraction peak (Fig. 4.1.4) increases with the increase in temperature from precursor (Fig. 4.1.4, no. 2) to sintered pellet (Fig. 4.1.4, no. 6), showing better crystallinity or larger amount of crystallite phase.

SEM and particle size distribution analysis

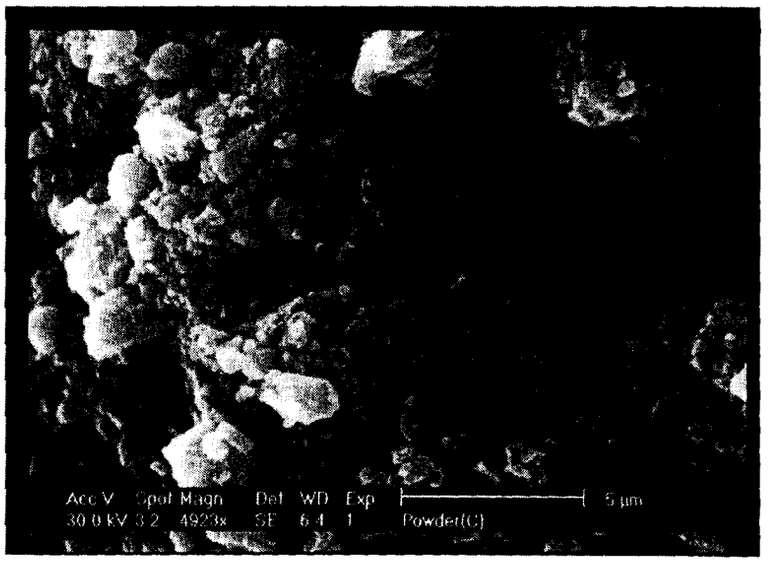

Fig. 4.1.7(a): SEM micrograph for co-precipitated powder calcined at 650°C

SEM micrographs show the morphological features of the powder calcined at 650°C (Fig. 4.1.7(a)) and a pellet sintered at 950°C (Fig. 4.1.8). For powder calcined at 650°C, fine particles are observed with the particle size less than 1 µm, which shown a tendency to form agglomerates.

The milled size of the powders calcined at 650°C is shown in Fig. 4.1.7(b). There are two peaks are observed in Fig. 4.1.7(b). The first peaks are generally shows that the milled size between 0.1 to 1.0 µm. For second peaks, the milled size between 10 to 100 µm, which may be due to ferrites powders agglomeration and other substances in water (Fig. 4.1.7(c)).

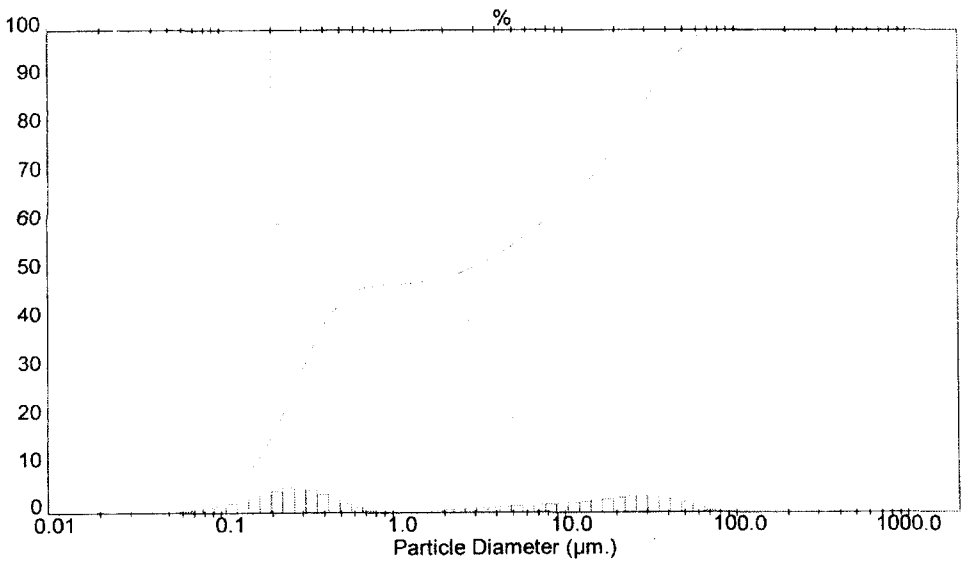

Fig. 4.1.7(b): Particle size distribution of the powder calcined at 650°C and milled for 6 hours

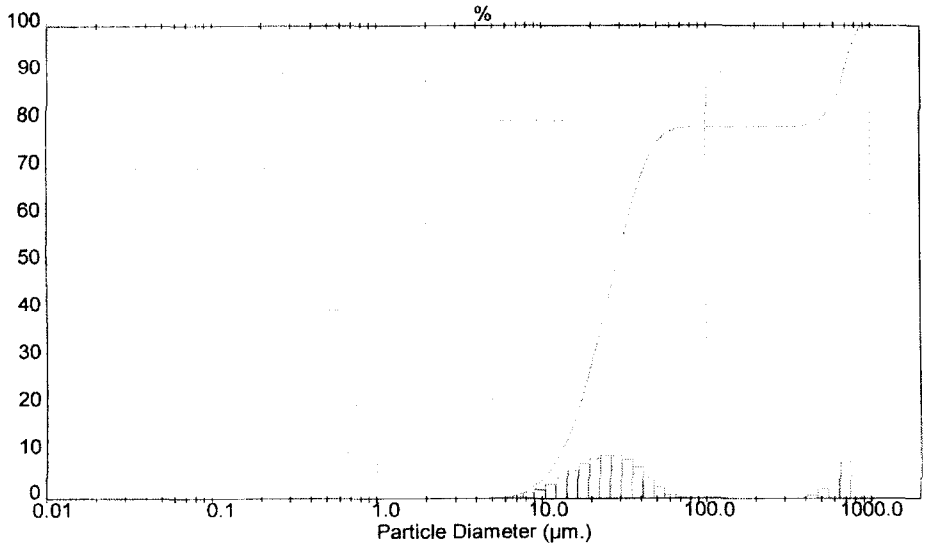

Fig. 4.1.7(c): Particle size distribution of the water

Fig. 4.1.7(c) shows the granularity distribution of the water. It can be seen that the particle size distribution of water is in the range of 10 to 100 μm. Therefore, it can be

seen that the milled size of powder calcined at 650°C is between 0.1 to 1.0 μm and this result is confirmed by SEM micrograph (Fig. 4.1.7(a)). For milled size between 10 to 100 μm, it can be considered as other substances in water or agglomerates of fine calcined powders, which also can be observed in SEM micrograph (Fig. 4.1.7(a)). Therefore, if only the particles whose granularities are small are considered, the milled size is less than 0.28 μm.

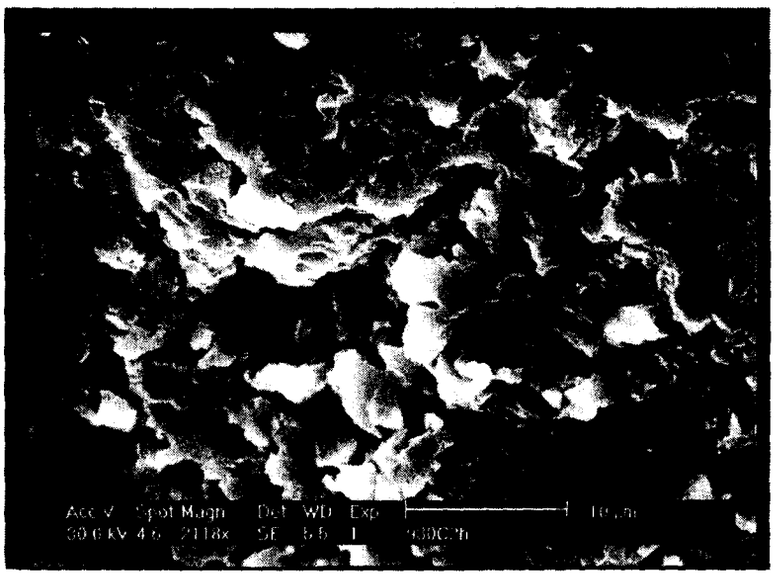

Fig. 4.1.8: SEM micrograph for compacted pellet sinter at 950°C

For the pellet sinter at 950°C (Fig. 4.1.8), SEM morphology shows that the fracture surface of the ferrite with porosity.

MgCuZn ferrite have been produced by the co-precipitation process from Mg^{2+}, Cu^{2+}, Zn^{2+} and Fe^{3+} chlorides solution. Synthesis of MgCuZn ferrite can be formed directly from dehydration process, which is produced directly from the 40 wash precursor and follow by dehydration at 180°C. However, further calcination is required to further improve the crystallinity of single spinel phase MgCuZn ferrite. The milled size of powder calcined at 650°C is about 0.28 μm.

4.1.2 The Investigation of Optimum Calcination Temperature

In this section, ferrites powders with different calcination temperatures of 600°C, 650°C, 700°C, 750°C, 800°C and 850°C were prepared. Pellets and toroids were each sintered at 900°C and 950°C.

Characterization of MgCuZn Ferrites

Calcination of MgCuZn ferrite was done at different temperatures ranging from 600°C to 850°C. The XRD diagram (Fig. 4.1.9) shows that as the calcination temperature increases, the diffraction peak broadening is decreased and the diffraction peak is sharpened.

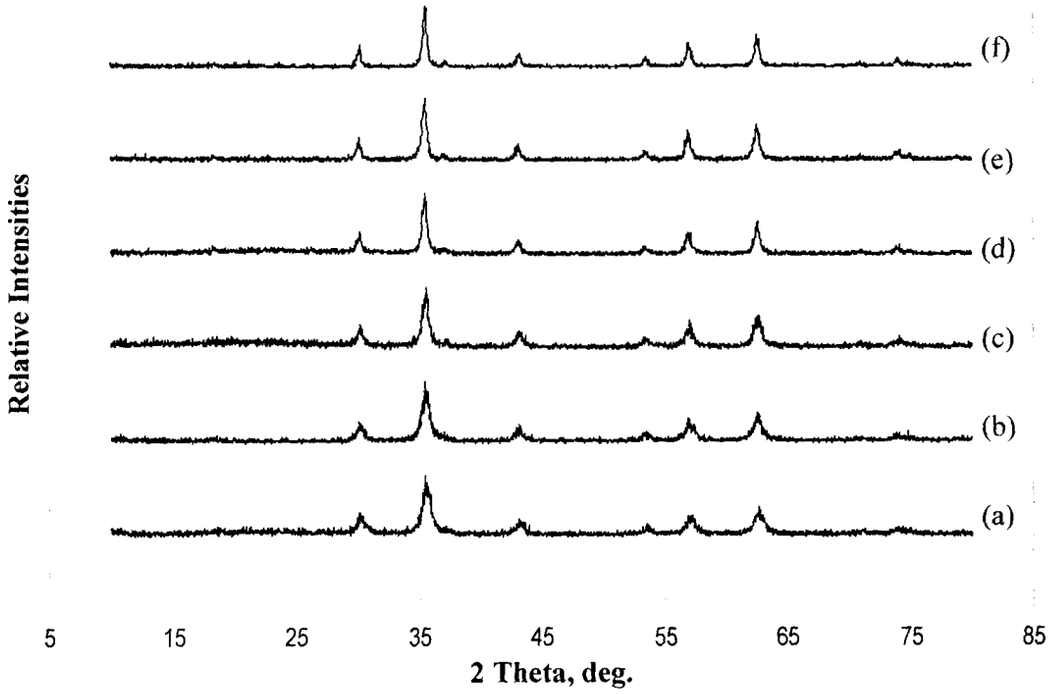

Fig. 4.1.9: XRD analysis for specimens calcined at (a) 600°C, (b) 650°C, (c) 700°C, (d) 750°C, (e) 800°C and (f) 850°C

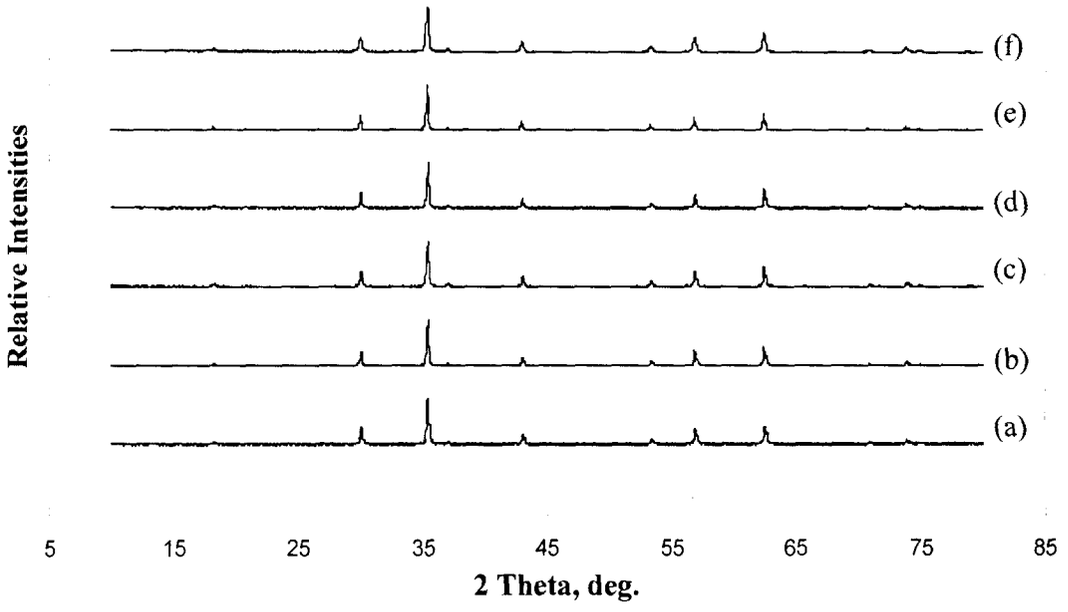

Fig. 4.1.10: XRD analysis for co-precipitated specimens sintered at 900°C with calcination temperature of (a) 600°C, (b) 650°C, (c) 700°C, (d) 750°C, (e) 800°C and (f) 850°C

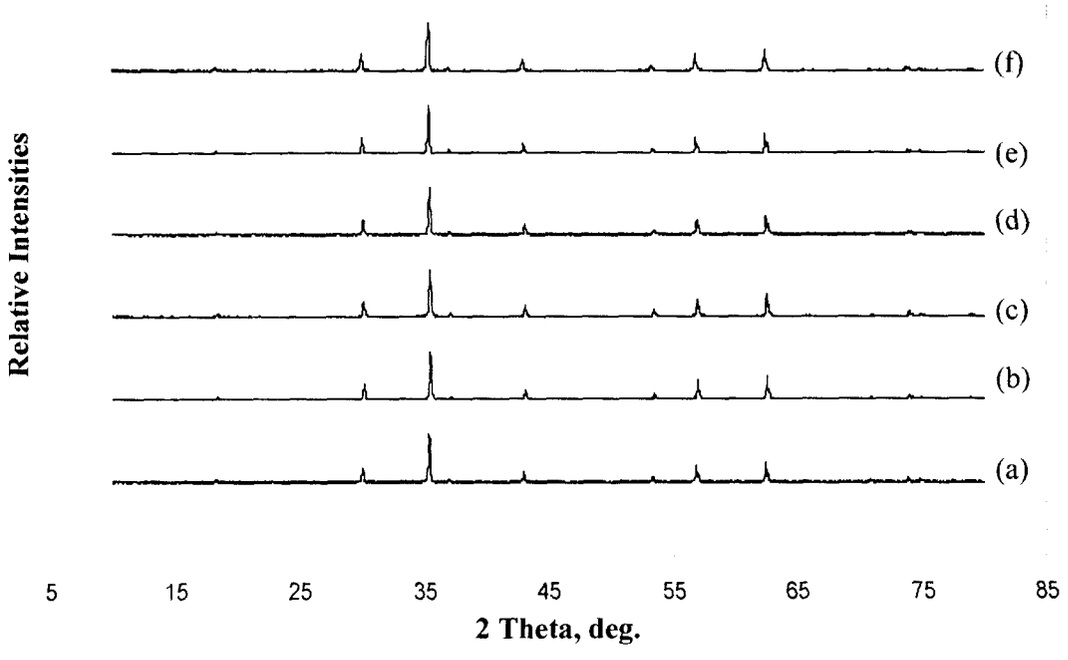

Fig. 4.1.11: XRD analysis for co-precipitated specimens sintered at 950°C with calcination temperature of (a) 600°C, (b) 650°C, (c) 700°C, (d) 750°C, (e) 800°C and (f) 850°C

Particle size will greatly affect the sinterability of the pressed powder. Fine particles will lead to a greater sintered density and a greater permeability [62]. Fine ferrite particles have a larger surface area and larger free energy. Since surface free energy is considered to be a driving force in the sintering process, the smaller ferrite particles tend to be well sintered. Therefore, suitable calcination temperature in ferrites processing is required in order to obtain a good surface area.

XRD patterns for specimens sintered at 900°C and 950°C with different calcination temperatures are shown in Fig. 4.1.10 and Fig. 4.1.11, respectively. XRD results show that with sintering taking place, complete formation of single spinel phase structure is observed with high sharpness of the major peaks and highly narrowing of diffraction line, together with no extra peak or secondary phases are detected in the XRD peaks. According to Shi et al. [61], the narrowing of diffraction line and high sharpness is due to a better order structure or an increase of grain size.

The fracture surface of specimens calcined at 650°C with sintering temperatures of 900°C and 950°C under SEM are shown in Fig. 4.1.12 and Fig. 4.1.13, respectively. Fig. 4.1.13 shows the formation of glassy phase under SEM, which will influence the characteristics and properties of MgCuZn ferrites. Glassy phase can increased densification, but not necessarily increased density. As compared to Fig. 4.1.12, Fig. 4.1.13 shows a higher degree of densification because of the higher sinterability observed. As the sintering temperature is increased, the number of pores is decreased due to the increased densification. Therefore, a higher density can be expected from the specimens with a sintering temperature of 950°C as compared to those specimens with a sintering temperature of 900°C.

Grain sizes are difficult to obtain because the grains are difficult to identify. Although it is difficult to determine the grain size, however, Fig. 4.1.12 and Fig.

4.1.13 show that a non – uniform distribution of pores and grain size can be observed with some agglomerated grains.

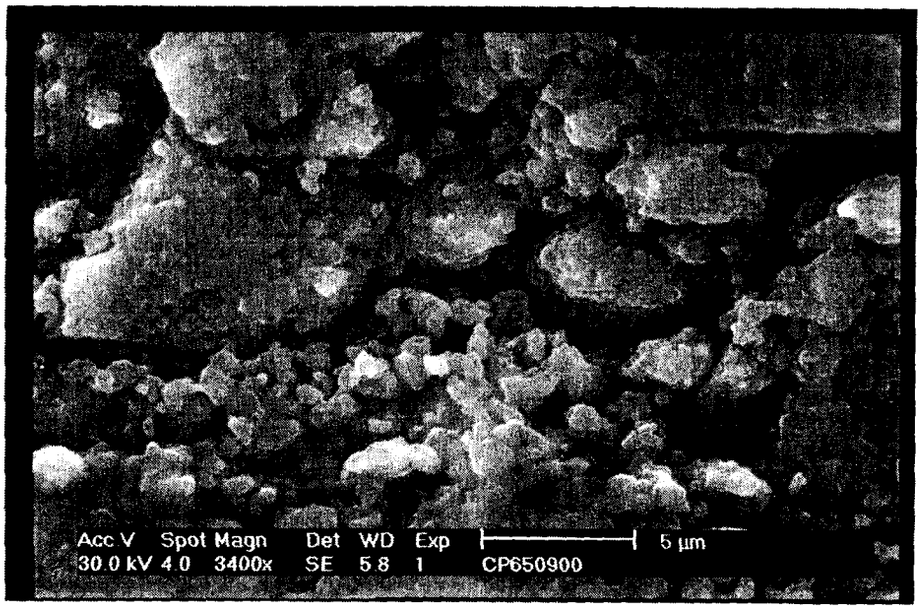

Fig. 4.1.12: SEM micrograph of the fracture surfaces of a specimen calcined at 650°C and sintered at 900°C

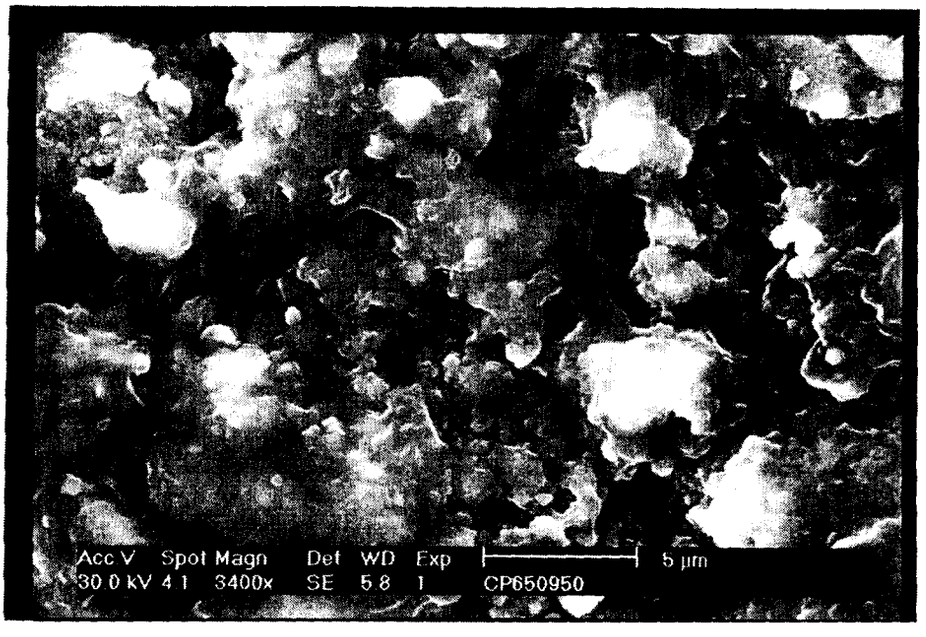

Fig. 4.1.13: SEM micrograph of the fracture surface of a specimen calcined at 650°C and sintered at 950°C

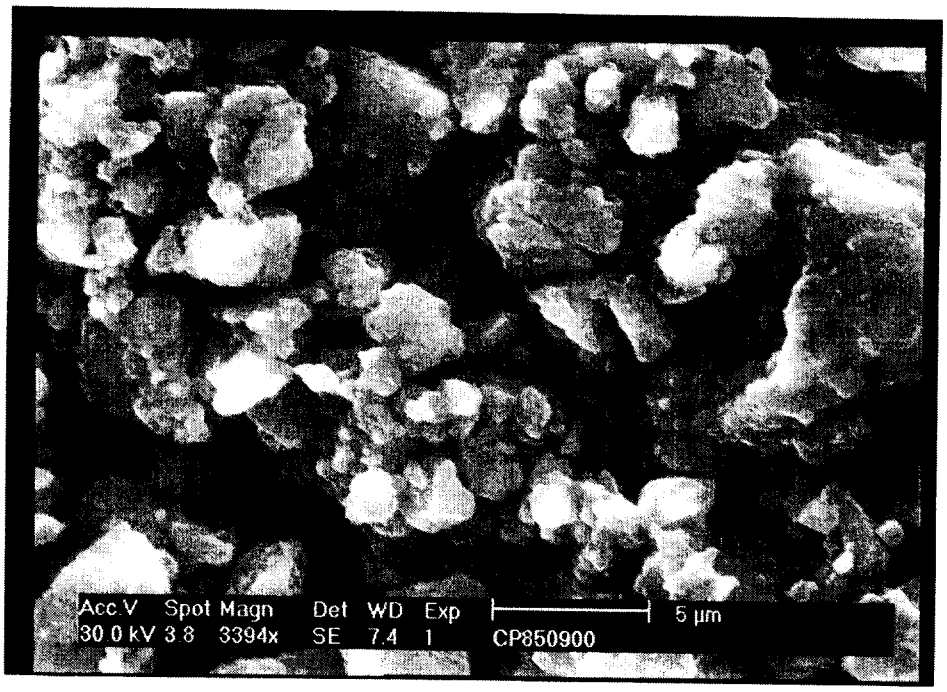

Fig. 4.1.14: SEM micrograph of the fracture surface of a specimen calcined at 850°C and sintered at 900°C

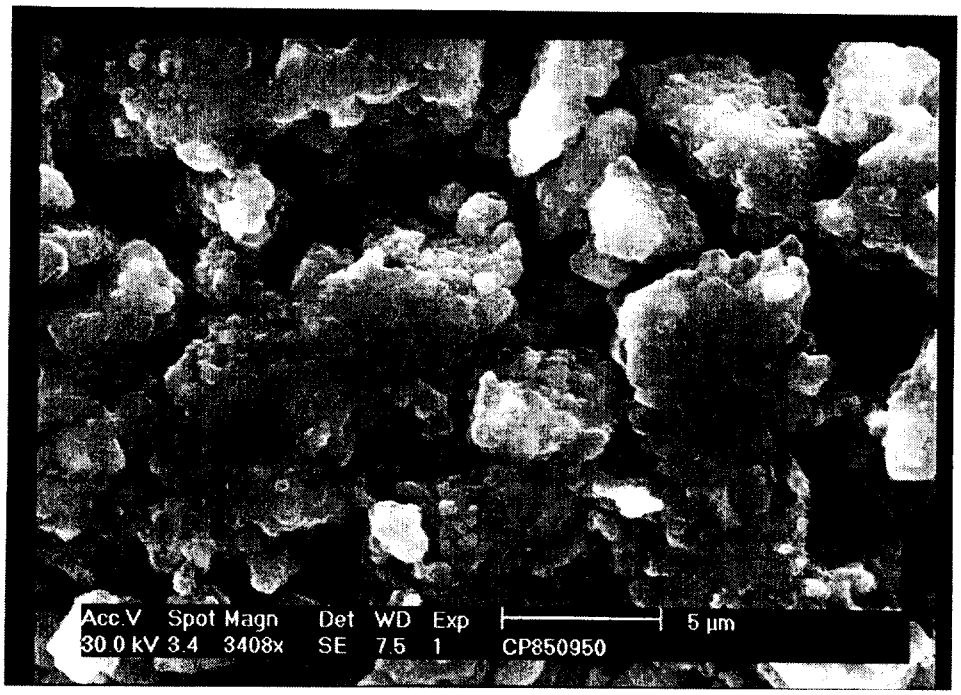

Fig. 4.1.15: SEM micrograph of the fracture surface of a specimen calcined at 850°C and sintered at 950°C

The SEM micrograph for specimen calcined at 850°C with sintering temperature of 900°C (Fig. 4.1.14) and 950°C (Fig. 4.1.15) shows lesser sinterability and high amount of porosity as compared to those calcined at 650°C with sintering temperature of 950°C (Fig. 4.1.13). This result is predicted due to the particle coarsening as calcination temperature exceeded an optimum temperature. Coarse particles will affect the densification during sintering. It can be expected that a large amount of thermal energy is required to sinter coarse particles, thus, low temperature sintering is considered to be difficult and there is less densification.

Densification and Electromagnetic Measurements

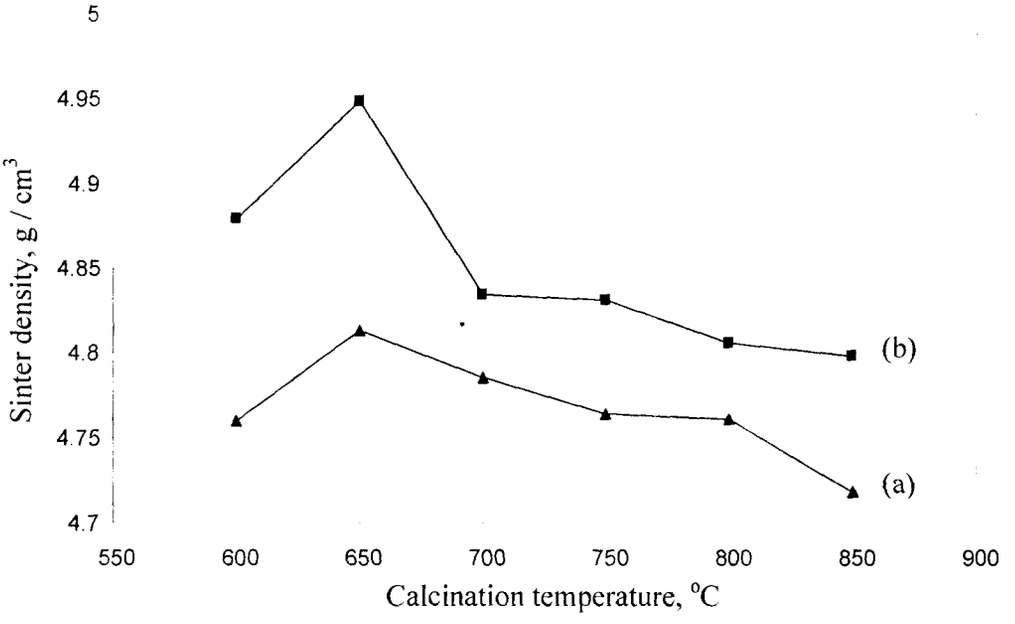

Fig. 4.1.16: Density measurements for specimens with different calcination temperatures and a sintering temperature of (a) 900°C and (b) 950°C

Fig. 4.1.16 shows the variation of the sintered density of MgCuZn ferrites with different calcination and sintering temperatures. It is indicated that both specimens sintered at 900°C and 950°C have an optimum sintered density and lowest porosity

(Fig. 4.1.17) at a calcination temperature of 650°C. The densification increases from 600°C to 650°C and then decreases with increasing calcination temperature.

The milled size of the calcined ferrites increases when the calcination temperature is raised. Therefore, a large amount of thermal energy is required to sinter the particles. Thus, low temperature sintering is considered to be difficult.

According to Nakahata et al. [22] and Murthy [20], powders calcined at different temperatures require different sintering temperatures to achieve a particular amount of shrinkage during firing. Therefore, densification is not only affected by the sintering temperature but also by the calcination temperature because different surface areas will be produced.

It can be observed that a calcination temperature of 650°C produces the highest density (4.95 g / cm^3) at a sintering temperature of 950°C. This is confirmed by the microstructure (Fig. 4.1.12 and 4.1.13), which indicates that the fracture surface of specimens sintered at 950°C is denser and less porous than the specimens sintered at 900°C. The porosity for specimens calcined at 650°C and sintered at 950°C is about 2 % (Fig. 4.1.17). However, SEM micrograph (Fig. 4.1.13) shows that big pores are present. Pores are divided into open pores and close pores. Fracture surface mainly referred to open pores. Therefore, the 2 % porosity is to be referred to close pores. Furthermore, glassy phase may improve the densification of the specimens calcined at 650°C and sintered at 950°C.

Density, porosity and grain size are important parameters, which will greatly affect the electromagnetic properties of MgCuZn ferrites. Ferrites are polycrystalline in microstructure. By increasing the sintering temperature, [illegible]tion of sintered ferrites occurred leading to a higher number of atoms cc [illegible] magnetic moment per unit volume [63]. Thus, the magnetic property will b[illegible]

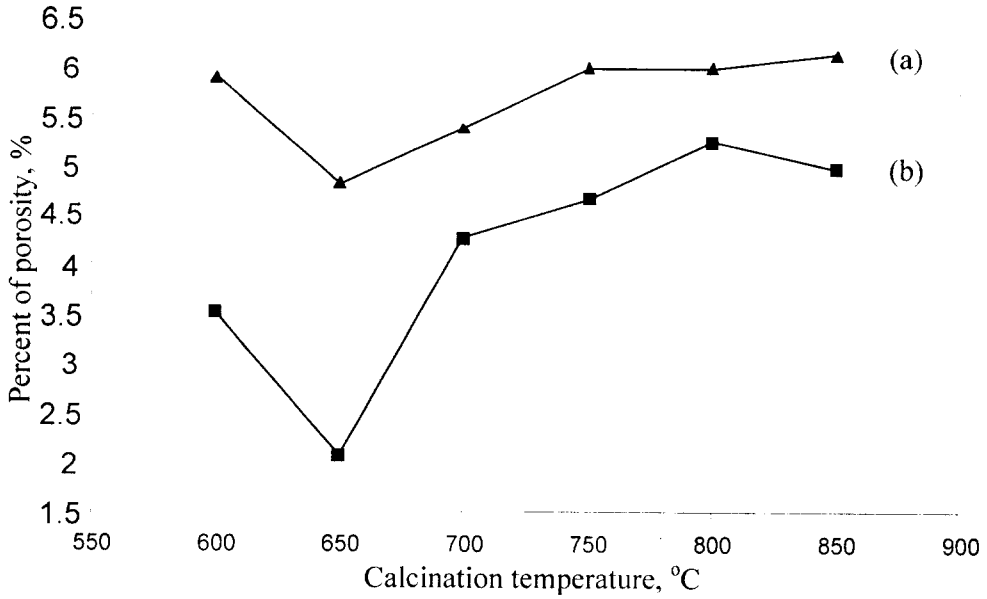

Fig. 4.1.17: Porosity measurement for specimens with different calcination temperatures and a sintering temperature of (a) 900°C and (b) 950°C

Fig. 4.1.18 and Fig. 4.1.19 show the initial permeability and quality factor as a function of calcination temperature for specimens sintered at 900°C and 950°C. It is clearly seen that the initial permeability and quality factor increase up to a calcination temperature of 650°C, where optimum initial permeability and quality factor are observed for both sintering temperatures. However, the properties started to deteriorate as the calcination temperature exceeded 650°C.

It is well known that initial permeability and quality factor depend on grain size, porosity, chemical composition and the presence of second phases [64]. Since there are no differences in chemical composition and in the absence of any second phases show in XRD analysis (Fig. 4.1.9, 4.1.10 and 4.1.11), the initial permeability and quality factor may be expected to be affected by grain size, porosity and density.

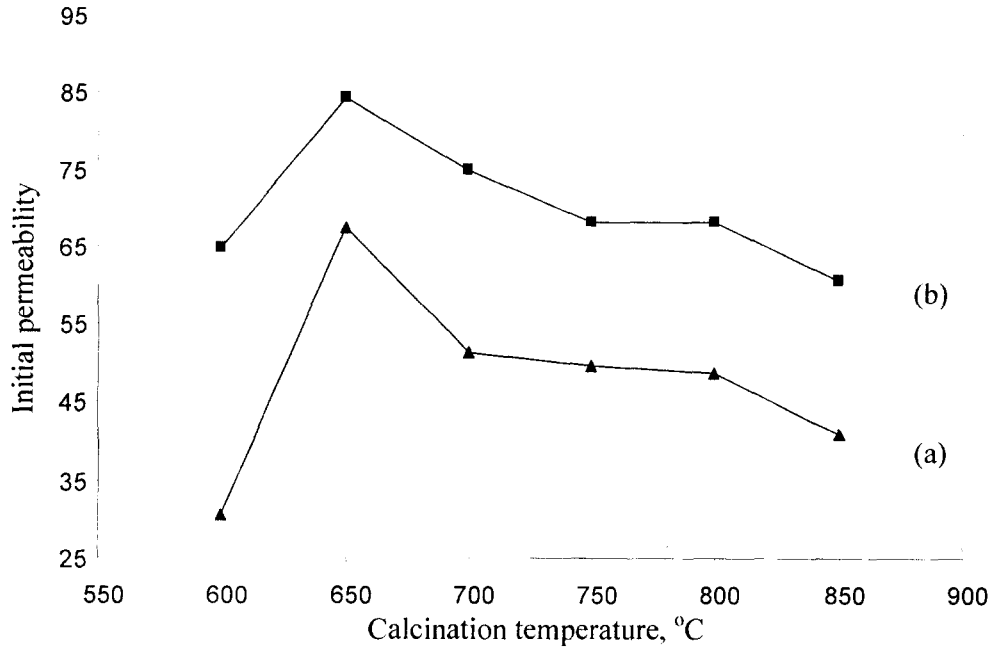

Fig. 4.1.18: Initial permeability (at 100 kHz) for specimens with different calcination temperatures and a sintering temperature of (a) 900°C and (b) 950°C

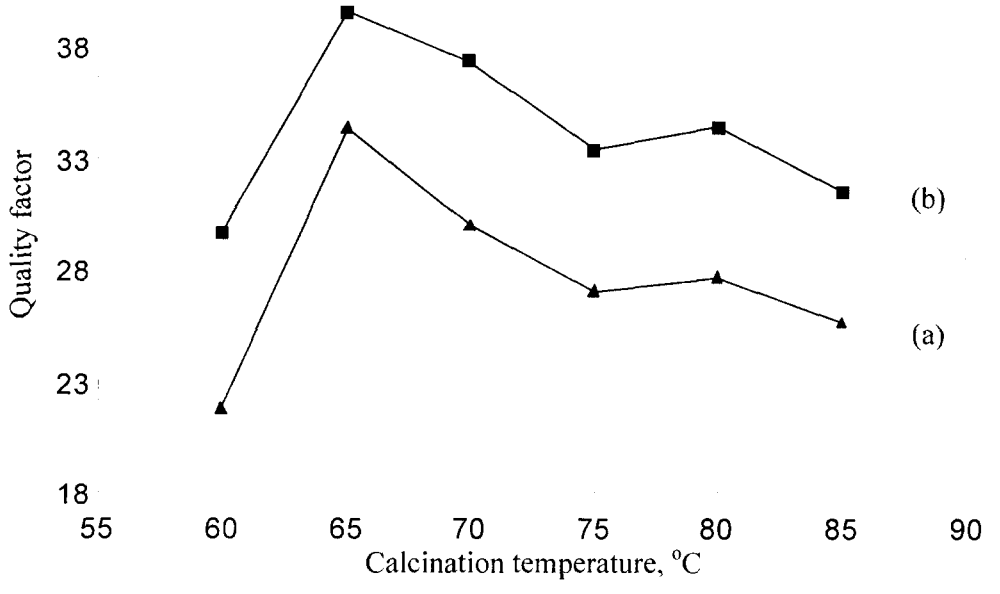

Fig. 4.1.19: Quality factor (at 100 kHz) for specimens with different calcination temperatures and a sintering temperature of (a) 900°C and (b) 950°C

According to Bhosale et al. [65], initial permeability could be resolved into two types of mechanism, which are

a. Contribution from spin rotation magnetization.
b. Contribution from domain – wall motion.

Nakamura [62] found that the domain wall motion starts to decrease at lower frequencies and the spin rotation magnetization remains in higher frequency regions. However, the contribution from spin rotation magnetization was found to be smaller than domain – wall motion [38].

Globus suggested that domain wall motion may be affected by the grain size and sintered density, which is enhanced by an increase of the grain size [66]. Fig. 4.1.16, Fig. 4.1.18 and Fig. 4.1.19 shows the same trend. Therefore, initial permeability and quality factor may be expected to increase with an increase of density and grain size, together with the reduction of porosity.

The presence of porosity could effectively pin the domain wall motion and cause a reduction in initial permeability and quality factor. Thus, by removal of domain wall pinning sites through the increase in grain size and improvement of densification, the grain boundary area is decreased, causing an increase in initial permeability and quality factor.

The variation of the DC electrical resistivity with calcination and sintering temperature is illustrated in Fig. 4.1.20, which shows that when the calcination temperature increases until 650°C, the DC electrical resistivity will decrease and reach a minimum for both sintering temperature of 900°C and 950°C. However, the DC electrical resistivity started to increase for calcination temperatures above 650°C for both sintering temperatures. These indicate that the specimen calcined at 650°C

shows the lowest DC electrical resistivity. It also indicates that specimens with a higher sintering temperature have a lower resistivity.

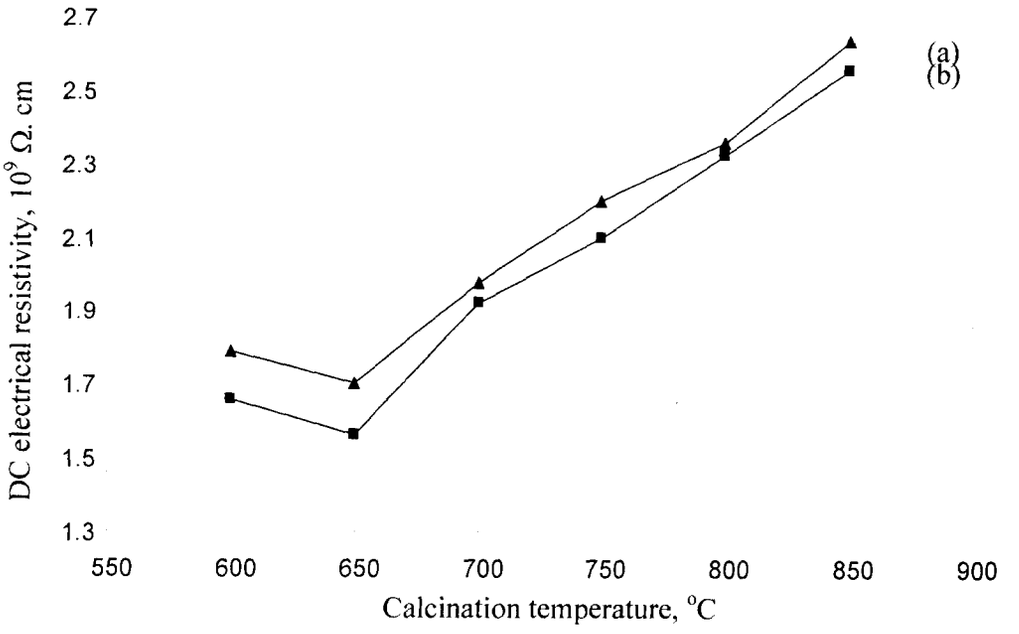

Fig. 4.1.20: DC electrical resistivity measurement for specimens with different calcination temperatures and a sintering temperature of (a) 900°C and (b) 950°C

Comparing Fig. 4.1.17 and Fig. 4.1.20, it is seen that material with a higher porosity has a higher DC electrical resistivity. When the porosity is increased, the number of pores, vacancies and scattering centres for the electrical charge carriers increases, which will cause the increase in DC resistivity.

It has also been reported that the resistivity of a polycrystalline ferrite is increased with a decrease in grain size [47]. Ferrites of small grain size have large area of grain boundary, which will trap imperfections, such as porosity, dislocation, impurities and any secondary phases. The grain boundary will act as a barrier to the flow of electrons. Therefore, smaller grains indicate the reduction in grain–to–grain surface contact area and cause the reduction in electron flow and increase in resistivity value.

Therefore, DC electrical resistivity may be expected to be influenced by non – conductive imperfections (such as porosity) and grain size.

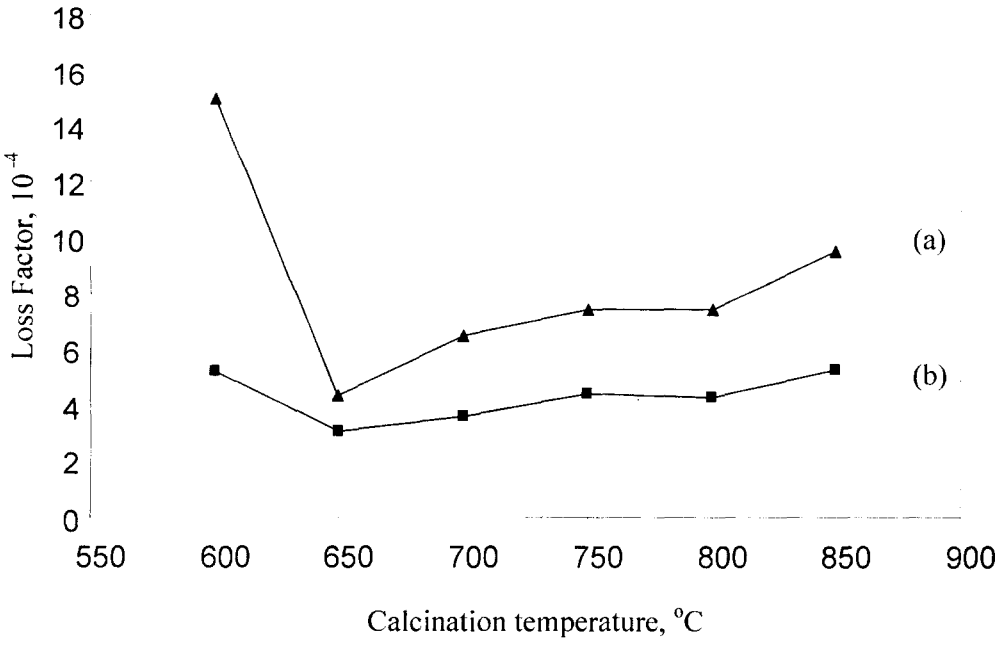

Fig. 4.1.21: Loss factor measurement for specimens with different calcination temperatures and a sintering temperature of (a) 900°C and (b) 950°C

The loss factor is important for multilayer chip inductors. In general, the loss factor values (Fig. 4.1.21) obtained are in the order of 10^{-4}. The loss factor indicates the magnetic losses, which are divided into hysteresis loss, eddy – current loss and residual loss. The lower the loss factor, the better the ferrite is.

The frequency that is used in this research is 100 kHz. When the frequency is lower than 500 kHz, the residual loss can be ignored [67]. The eddy – current loss is reciprocal to the resistivity and proportional to the square of the frequency. Since the resistivity value obtained is high, in the order of 10^9, the eddy – current loss is considered to be negligible. Thus, the total magnetic losses are considered to be predominantly hysteresis loss. The hysteresis loss is sensitive to microstructural homogeneity and to the presence of second phases. The present of second phases is

not detected by XRD results (Fig. 4.1.9, 4.1.10 and 4.1.11). Hence, any increase of the porosity content will increase losses.

From Fig. 4.1.21, a calcination temperature of 650°C for both sintering temperature of 900°C and 950°C shows a lower loss factor. The sintering temperature of 950°C will give a minimum loss factor. The decrease in loss factor may be due to the decrease of domain wall pinning and grain boundary. Thus, the reduction in losses might be due to the reduction in porosity.

The specimens prepared from powder with a calcination temperature of 650°C shows the absence of second phases, highest density, lowest porosity, highest initial permeability and quality factor, good DC electrical resistivity and lowest loss factor value. Good electromagnetic properties are not only important in multilayer chip inductors but also for telecommunication purposes. For telecommunication application, ferrites with a high quality factor are desired in the high frequency range. Therefore, a calcination temperature of 650°C is selected for the investigation on optimum sintering temperature by co-precipitation process.

4.1.3 The Investigation of Optimum Sintering Temperature Characterization of MgCuZn Ferrites

The fracture surface of specimens calcined at 650°C with sintering temperatures of 900°C, 930°C and 950°C are shown in Fig. 4.1.22, Fig. 4.1.23 and Fig. 4.1.24, respectively. As compared to Fig. 4.1.22, Fig. 4.1.23 and Fig. 4.1.24 shows a higher degree of densification because of the higher sinterability and lower porosity are observed.

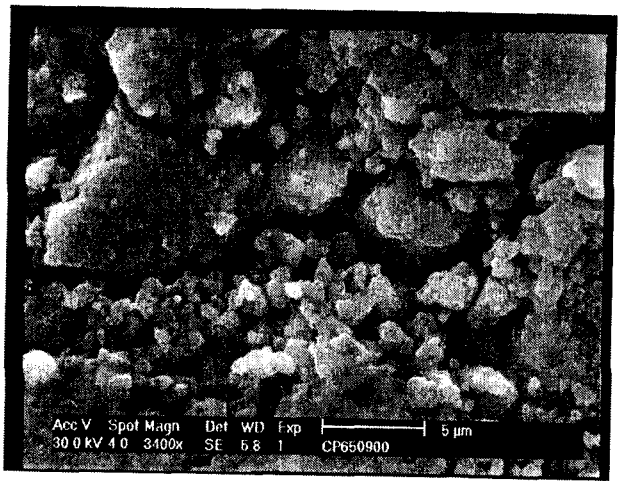

Fig. 4.1.22: SEM micrograph of the fracture surfaces of a specimen calcined at 650°C and sintered at 900°C

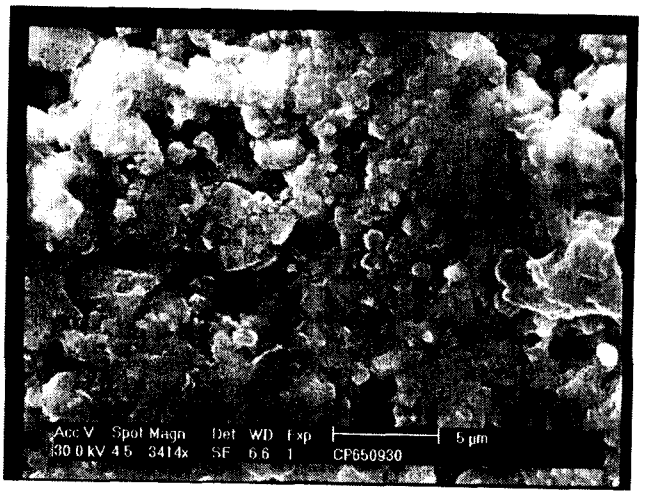

Fig. 4.1.23: SEM micrograph of the fracture surfaces of a specimen calcined at 650°C and sintered at 930°C

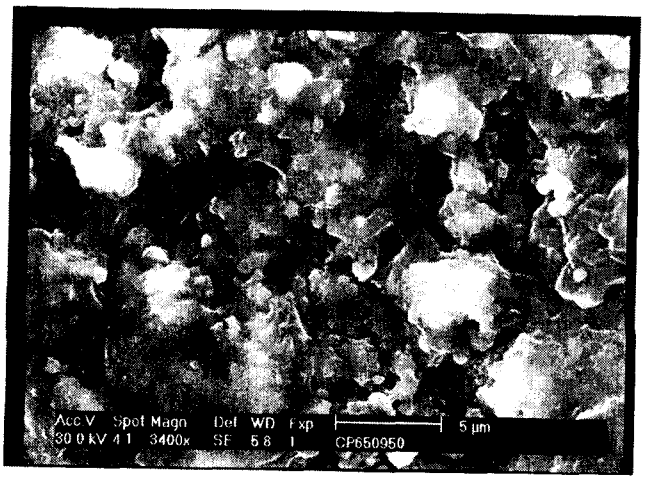

Fig. 4.1.24: SEM micrograph of the fracture surfaces of a specimen calcined at 650°C and sintered at 950°C

Grain sizes are difficult to obtain because the grains are difficult to identify. Although it is difficult to determine the grain size, however, Fig. 4.1.22, Fig. 4.1.23 and Fig. 4.1.24 show that a non – uniform distribution of pores and grain size can be observed with some agglomerated grains.

Densification and Electromagnetic Measurements

Table 4.1.1: Sinter density and porosity measurement for specimens with calcination temperature of 650°C and a sintering temperature of 900°C, 930°C and 950°C

Sintering Temperature, °C	Sinter density, g / cm^3		Porosity, %
	Theoretical	sintered	
900	5.0565	4.8129	4.8176
930	5.0664	4.9669	1.9639
950	5.0520	4.9477	2.0645

The sinter density and porosity of sintered MgCuZn ferrites with sintering temperatures of 900°C, 930°C and 950°C using co-precipitation process are shown in Table 4.1. The sintered density has been significantly increased until sintering temperature of 930°C and then a small reduction in sintered density is observed from sintering temperature of 930°C to 950°C. The small reduction in sintered density is expected to be attributed by the increase in intragranular porosity resulting from discontinuous grain growth. Overall, MgCuZn ferrites materials with co-precipitation process have a sintered density higher than 95% of the theoretical density calculated from the XRD results.

It can be seen that the porosity for specimen sintered at 930°C is relatively low. However, SEM micrograph (Fig. 4.1.23) shows that big pores are present. Pores are

divided into open pores and close pores. Fracture surface mainly referred to open pores. Therefore, the about 2 % porosity is predicted to be referred to close pores.

According to Mangalaraja et al. [68], the saturation magnetization (M_S) value increases with sintering temperature and the relation between M_S and porosity and density is expressed as:

$$M_S = (1 - P)\, \delta_S\, d_S \quad \text{.....(4.1.2)}$$

Where, P is prorosity, d_S is density, δ_S is M_S (obs.) / M_S (sat.).

From the equation (4.1.2), it is clear that saturation magnetization increases with decrease in porosity. Variations of initial permeability of MgCuZn ferrites were also influenced by saturation magnetization, which can be related by the following equation [39]:

$$\mu_i\, a\, (M_S)^2 / (a\, K + b\, \lambda\, \sigma) \quad \text{.....(4.1.3)}$$

Which, μ_i is initial permeability, σ is Inner stress, K is Crystal magnetic anisotropy constant and λ is Magnetostriction constant.

According to equation (4.1.3), initial permeability is proportional to the square of the saturation magnetization. Therefore, it can be expected that the reduction in porosity will cause the increase in initial permeability.

Fig. 4.1.25 shows the initial permeability values versus frequency for specimens calcined at 650°C with sintering temperature of 900°C, 930°C and 950°C, respectively. The initial permeability (at frequency between 10 to 100 kHz) of the specimens at sintering temperature of 900°C, 930°C and 950°C appeared to be 67 – 69, 90 – 93 and 84 – 86, respectively. Overall, slight reduction in initial permeability is observed from low to high frequency.

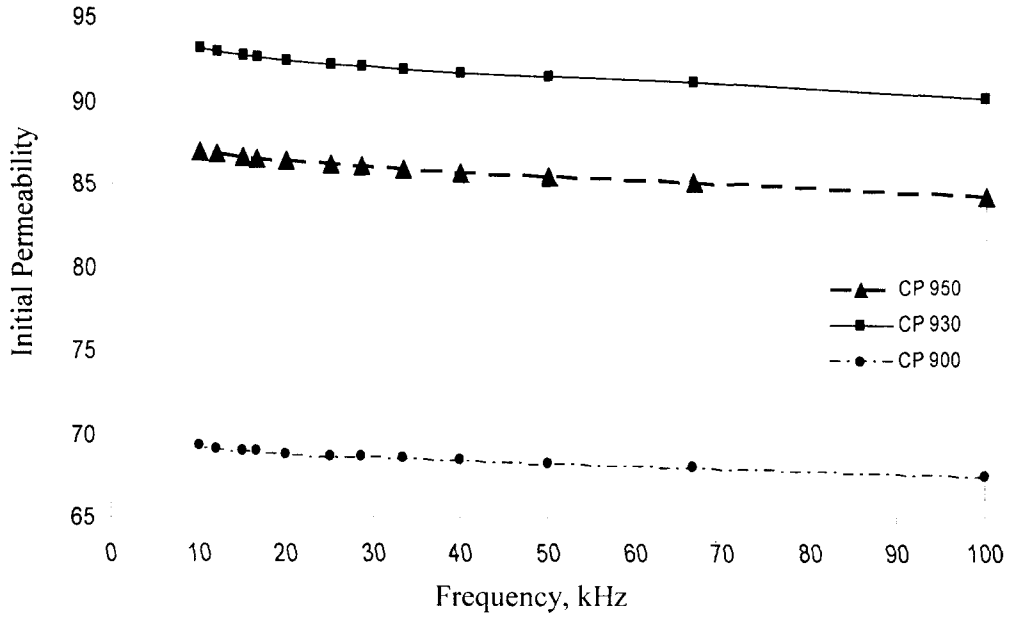

Fig. 4.1.25: Initial permeability measurement for specimens calcined at 650°C with sintering temperature of 900°C, 930°C and 950°C

As the sintering temperature is increased to 930°C, it could be seen that highest value of initial permeability is observed. However, the initial permeability of specimens sintered at 950°C decreases, which was probably due to the fact that, although the sizes of the grains are slightly increase, the permeability decreases due to the pinning effect which occurred when the magnetic wall moved. The presence of porosity will effectively pin the magnetic wall movement. From Table 4.1, it can be seen that specimens sintered at 930°C have the higher sintered density and lower porosity as compared to the one sintered at 950°C. Therefore, it could be expected that increase in porosity and reduction in sintered density will greatly reduce the initial permeability value.

Other than porosity and sintered density, the degradation of initial permeability due to the increase in sintering temperature from 930°C to 950°C can be explained in terms of copper ions. According to Tsay et al. [69], one of the possible factors is the

modification in oxidation of the copper ions. It should be noted that Cu^{2+} ions are magnetic and will contribute large magneto–anisotropy to the materials, whereas the Cu^{1+} ions are non–magnetic and are expected to insignificantly alter the intrinsic magnetic properties of the materials. Therefore, the decrease in initial permeability with increasing sintering temperature is suspected to be attributed by the modification of the Cu^{2+} / Cu^{1+} ion ratio. This argument is supported by the fact that the initial permeability value of the specimens varied only with the sintering temperature used for densification, but is independent of the soaking time used for sintering [69]. This is in accordance with the fact that the oxidation state of Cu^{n+} ions is determined only by the temperature, which the materials experienced [70].

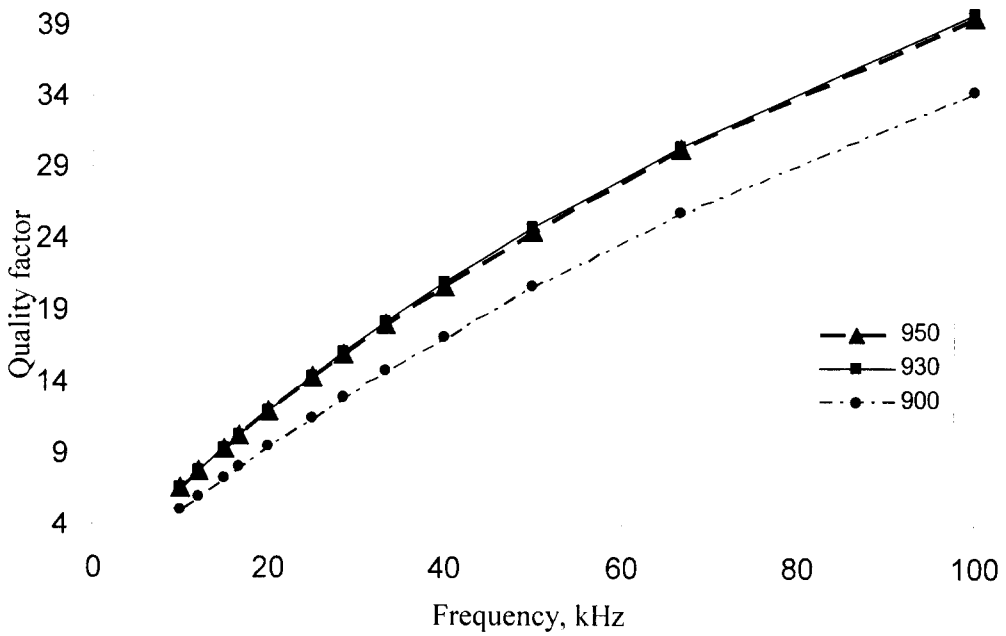

Fig. 4.1.26: Quality factor measurement for specimens calcined at 650°C with sintering temperature of 900°C, 930°C and 950°C

It can be observed from Fig. 4.1.26 that the quality factor increases with an increase in sintering temperature. However, the specimens with sintering temperature of

930°C and 950°C have almost the same quality factor throughout the frequency range from 10 to 100 kHz.

The dependence of the quality factor on the sintering temperature and frequency was different from that of the initial permeability (Fig. 4.1.25). The quality factor is increased from low frequency to high frequency for specimens with sintering temperature of 900°C, 930°C and 950°C. However, for initial permeability, slight reduction in initial permeability is observed from low to high frequency.

It appears that quality factor of the specimens are increased with the increased in sintered densities values. The quality factor (at frequency between 10 to 100 kHz) of the specimens at sintering temperature of 900°C appear to be increased from 5 to 34, whereas for specimens sintered at 930°C and 950°C, the quality factor is increased from 6 to 39.

Generally, quality factor is considered in relation to frequency, inductance, type of winding conductor and the effective permeability of the core. Also, the quality factor (Q) of a magnetic component is defined by the following equation [33]:

$$Q = (2 \pi f L) / R_S \qquad (4.1.4)$$

Where, f is frequency, L is inductance and R is series resistance (ohms).

From equation (4.1.4), quality factor is proportional to frequency. Therefore, the higher the frequency, higher the quality factor will be obtained and it can be observed by Fig. 4.1.26.

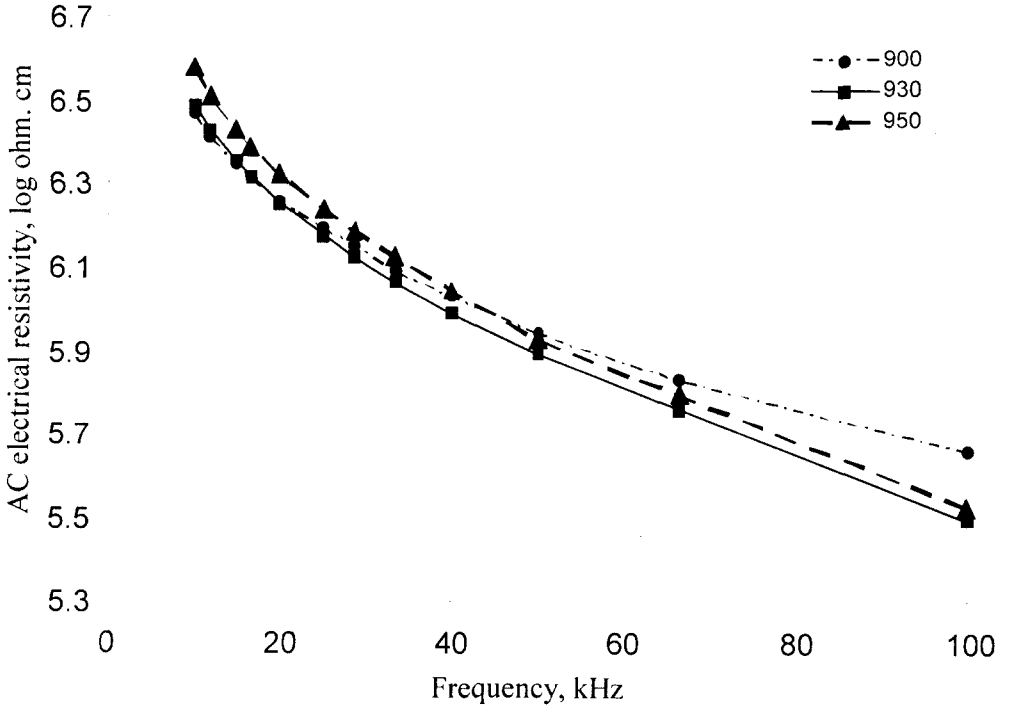

Fig. 4.1.27: AC electrical resistivity measurement for specimens calcined at 650°C with sintering temperature of 900°C, 930°C and 950°C

Fig. 4.1.27 shows the effect of frequency and sintering temperature on the AC electrical resistivity of MgCuZn ferrite measured at room temperature. All the specimens show a trend of reduction from frequency of 10 kHz to 100 kHz.

Overall, throughout the frequency range from 10 kHz to 100 kHz, the specimen sintered at 930°C shows the lowers AC electrical resistivity, which is expected to be due to the low porosity. However, specimens sintered at 900°C and 950°C show different AC electrical resistivity dependent on the frequency that in used.

The resistivity of the ferrites in general depends on the density, porosity, grain size and chemical composition of the specimens. The decrease in AC electrical resistivity is attributed to the reduction in porosity, increase in density and increase in grain size. The decrease in AC electrical resistivity with the increase of sintering temperature has also been attributed to the increase of divalent iron content [71].

The conduction mechanism in ferrites is explained in terms of hopping of charge carriers between the Fe^{2+} and Fe^{3+} ions on octahedral sites. The increase in frequency enhances the hopping frequency of charge carriers, resulting in an increase in the conduction process and thereby a decrease in the resistivity. Ferrites are low mobility materials, and the increase in conductivity means that the mobility of charge carriers has increased, but not the number of charge carriers. Furthermore, at high frequency, the resistivity remains invariant with frequency, because the hopping frequency no longer follows the external field but rather, lags behind it.

The resistive grain boundaries were found to be more effective at lower frequencies while the conductive ferrites grains are more effective at higher frequencies [68]. These grain boundaries were formed by the superficial reduction or oxidation of the crystallites in the porous material as a result of their direct contact with firing atmosphere [72]. Also, the increase in AC electrical conductivity (σ'_{AC}) as frequency increases can be explained by the following equation [72]:

$$\sigma'_{AC} = (w \varepsilon' \tan \delta) / (4 \pi) \quad \text{.....(4.1.5)}$$

Where, w is ($2 \pi f$), f is frequency, ε' is real dielectric constant and $\tan \delta$ is dielectric loss.

From Fig. 4.1.27, it can be seen that specimens sintered at 900°C and 950°C have the same AC electrical resistivity value at about 45 kHz. Below the frequency of 45 kHz, the AC electrical resistivity of specimens sintered at 950°C is higher than specimens sintered at 900°C. It is suspected that the resistive grain boundary effect of specimens sintered at 950°C is more pronounce than those sinter at 900°C. However, above 45 kHz, the AC electrical resistivity of specimens sintered at 900°C is higher than specimens sintered at 950°C. It is suspected that the conductive ferrite grains of specimens sintered at 950°C is more pronounce than those sinter at 900°C

The microstructure also influences the resistivity of the sintered ferrite. Small and relatively uniform grain size leads to faster oxidation. Thus, it will reduce the probability of Fe^{2+} formation and cause the increase in resistivity [73].

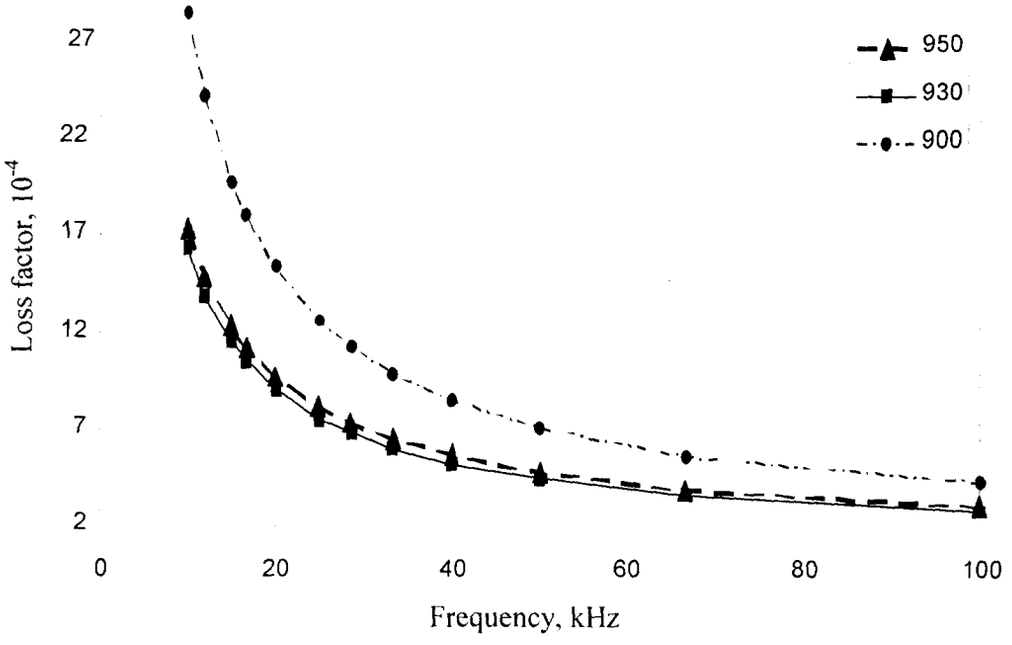

Fig. 4.1.28: Loss factor measurement for specimens calcined at 650°C with sintering temperature of 900°C, 930°C and 950°C

The loss factor is plotted against frequency in Fig. 4.1.28 for MgCuZn ferrites sintered at temperature of 900°C, 930°C and 950°C. From a frequency of 10 kHz to 100 kHz, the loss factor is observed to decrease and it is believed that it will reach a minimum level as the frequency increases to more than 100 kHz. In general, the loss factor is in the order of 10^{-4}. Specimens sintered at 930°C are found to exhibit the lowest loss factor as compared to others specimens and specimens sintered at 950°C have a loss factor close to those sintered at 930°C.

Sudden drop in loss factor from 10 to 30 kHz is not known as yet.

The loss factor values are known to depend on stoichiometry, density, grain size, Fe^{2+} content and structural homogeneity [74]. Each of these factors varies with composition and processing temperature. From Fig. 4.1.28, specimens sintered at 930°C have the lowers loss factor, which is predicted due to the highest density value and lowest porosity. Other than that, it might also be due to the compositionally and structurally more perfect than those sintered at 900°C and 950°C.

Generally, magnetic losses consist of hysteresis loss, eddy current loss and residual loss. Since the residual loss in ferrite is only important at very low induction levels or at high frequency (more than 500 kHz), the residual loss can be considered to be negligible [75]. Thus, the losses can be considered to be hysteresis loss and eddy current loss.

For ferrites to be useful as inductor materials, they should have high density, low porosity, high initial permeability, high quality factor, high resistivity and low loss factor over the frequency range of interest. Thus, specimens calcined at 650°C and sintered at 930°C would be preferred in this regard.

4.2 Synthesis of MgCuZn Ferrites by Mixed Oxide Route

4.2.1 The Investigation of Optimum Calcination Temperature

In the section, ferrites powders with different calcination temperature of 650°C, 700°C, 750°C, 800°C, 850°C and 900°C were prepared. Pellets and toroids were each sintered at 900°C and 950°C, according to different calcination temperature.

Characterization of MgCuZn Ferrites

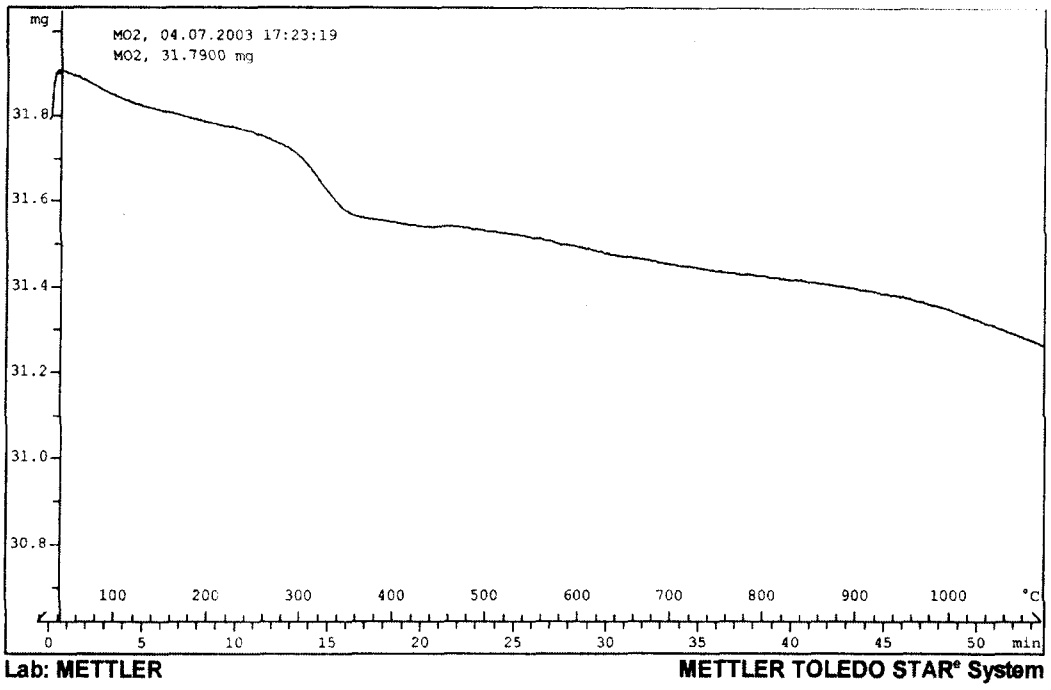

Fig. 4.2.1: TGA analysis for mixed oxide specimens after mixing and ball milling

Before calcination takes place, 31.79mg of mixed powder (after ball milling) was subjected to TGA and SDTA analysis. TGA analysis (Fig. 4.2.1) reveals that the mixed powders gradually lose weight from about 200°C to 400°C. Then, a small amount of weight loss is observed after a temperature of 400°C. Also, there is a small weight loss from room temperature to about 200°C.

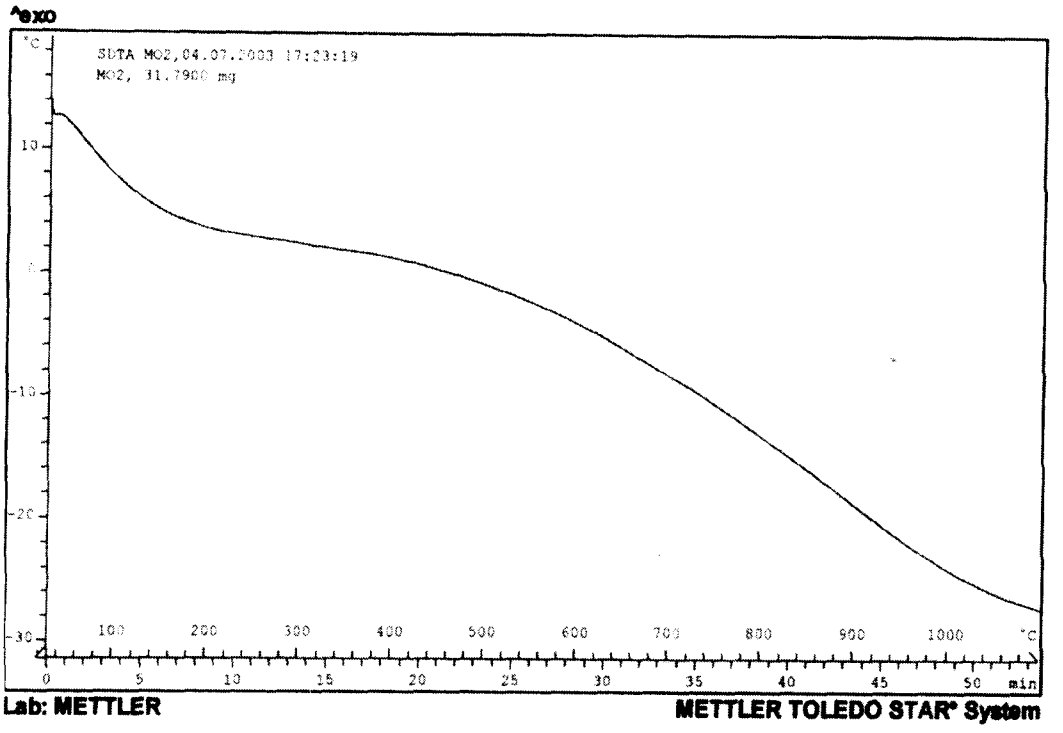

Fig. 4.2.2: SDTA analysis for mixed oxide specimens after mixing and ball milling

SDTA analysis (Fig. 4.2.2) shows that decomposition takes place from room temperature to about 200°C and then the decomposition occurs continuously.

From both TGA and SDTA analysis, it can be observed that dehydration occurs at a temperature of about 200°C. Although a loss in weight was observed from room temperature to 400°C (Fig. 4.2.1), XRD analysis (Fig. 4.2.3) indicates that formation of ferrite phase has not been completed as extra peaks are observed. Therefore, the mixed powders required further calcination in order to ensure complete formation of single spinel ferrite phase without any extra phases and improved crystallinity. Thus, the study of different calcination temperatures ranging from 650°C to 900°C has been done to analyze the effect of secondary phases, e.g., hematite (α - Fe_2O_3) [76] on the electromagnetic properties of MgCuZn ferrites synthesized by mixed oxide route.

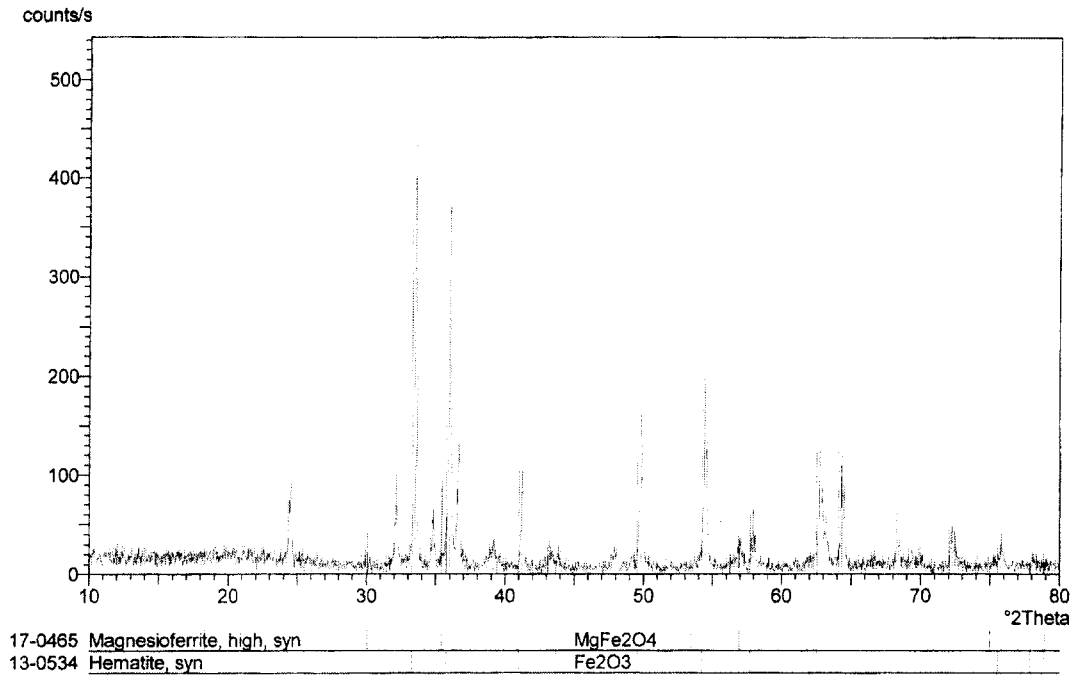

Fig. 4.2.3: XRD analysis for specimens calcined at 400°C

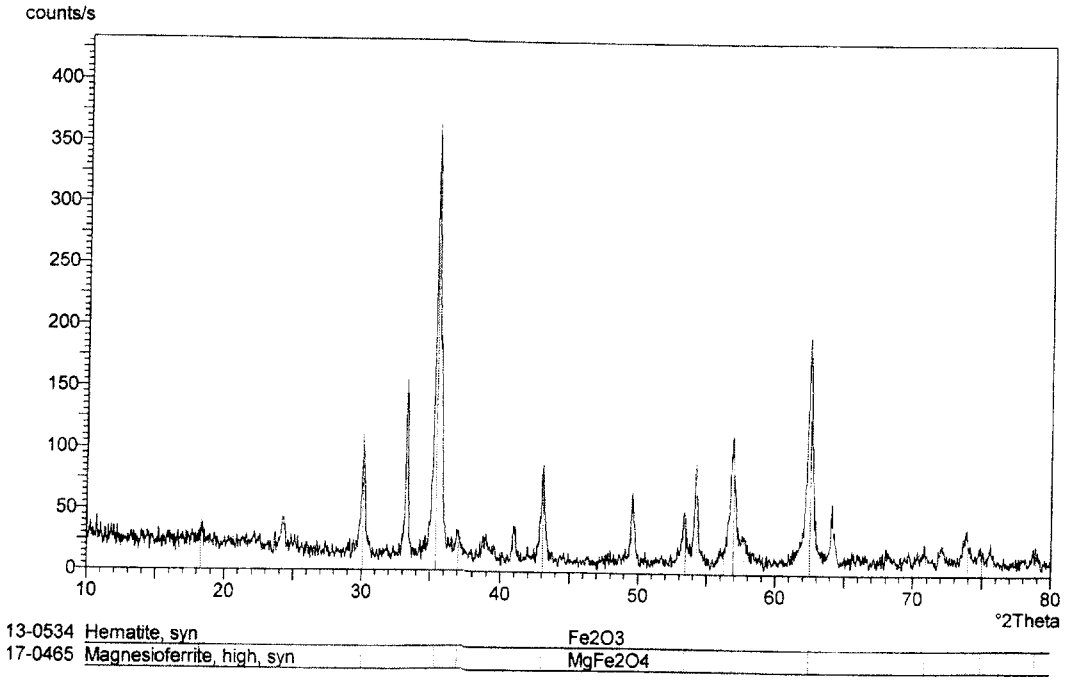

Fig. 4.2.4: XRD analysis for specimens calcined at 650°C

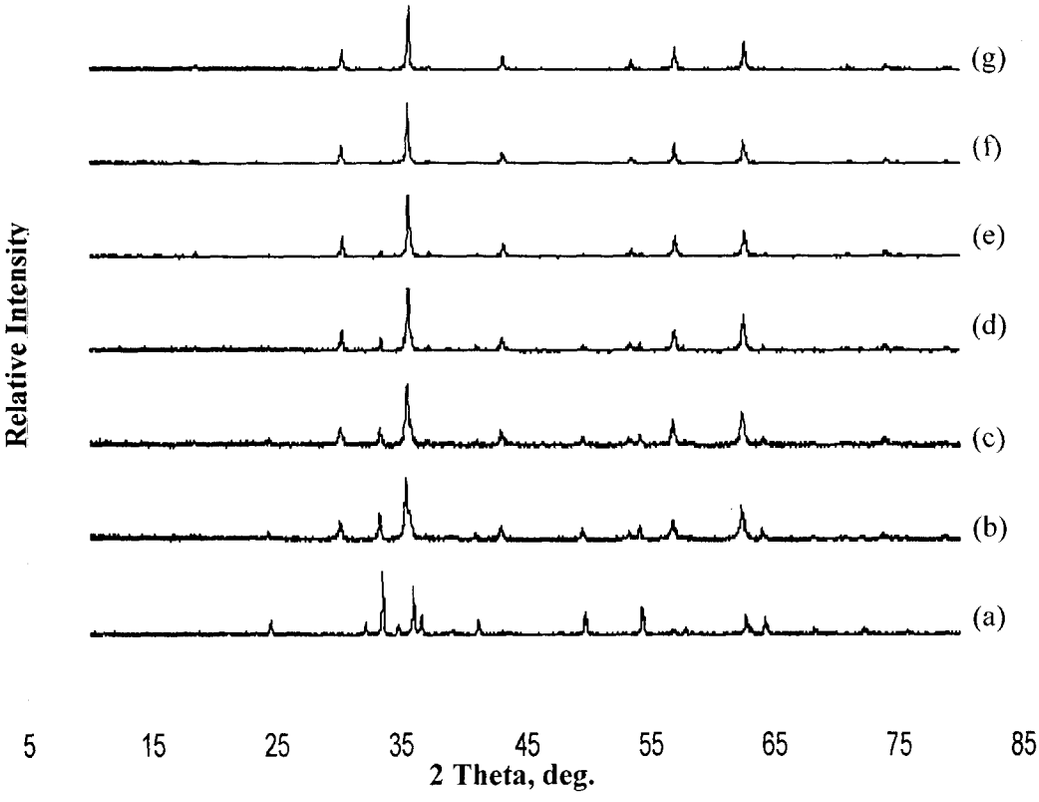

Fig. 4.2.5: XRD analysis for specimens calcined at (a) 400°C, (b) 650°C, (c) 700°C, (d) 750°C, (e) 800°C, (f) 850°C and (g) 900°C

XRD patterns (Fig. 4.2.4) of powders calcined at 650°C indicate that the powder consists of spinel crystal structure of MgCuZn ferrites with the characteristic reflections of magnesium ferrite. The peaks at $2\theta \approx 18.2^{\circ}$, 30°, 35.5^{0}, 37°, 43°, 53.5°, 57°, 62.5°, 70.5°, 74.5°, 75° and 79° appeared indicating the formation of a crystalline phase. However, this specimen also contains a secondary phase which has been identified as hematite (α - Fe_2O_3) phase. The peaks at $2\theta \approx 24^{\circ}$, 33°, 35.7°, 41°, 49°, 54°, 64°, 72° and 75.5° appeared to be from the hematite phase.

The XRD patterns of specimens calcined at 400°C, 650°C, 700°C, 750°C, 800°C, 850°C and 900°C for 2 hours are shown in Fig. 4.2.5. Except for the specimen with a calcination temperature of 400°C, all the specimens match well to the characteristic

reflections of magnesium ferrite with hematite as secondary phase. The XRD diffraction lines for hematite are reduced gradually for calcination temperatures from 650°C to 850°C and undetected at a temperature of 900°C. The relative intensity of the diffraction lines assigned to hematite phase tends to decrease sharply with the increase of the calcination temperature. Therefore, it can be observed that a calcination temperature above 850°C is required in mixed oxide route for the formation of single spinel phase.

The XRD spectra (Fig. 4.2.5) also show that as the calcination temperature increases from 650°C to 900°C, the diffraction peak broadening is decreased and the diffraction peak is sharpened. According to Shi et al. [61], the narrowing of diffraction line and high sharpness is due to a better order structure or an increase of grain size.

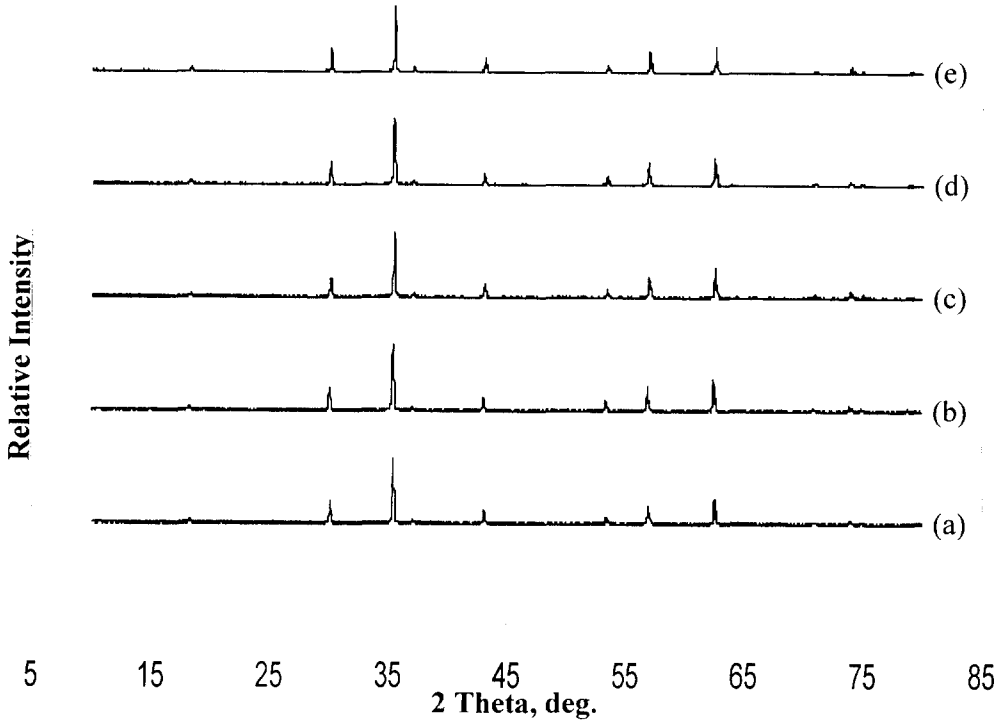

Fig. 4.2.6: XRD analysis for specimens sintered at 900°C with calcination temperature of (a) 650°C, (b) 700°C, (c) 750°C, (d) 800°C and (e) 850°C

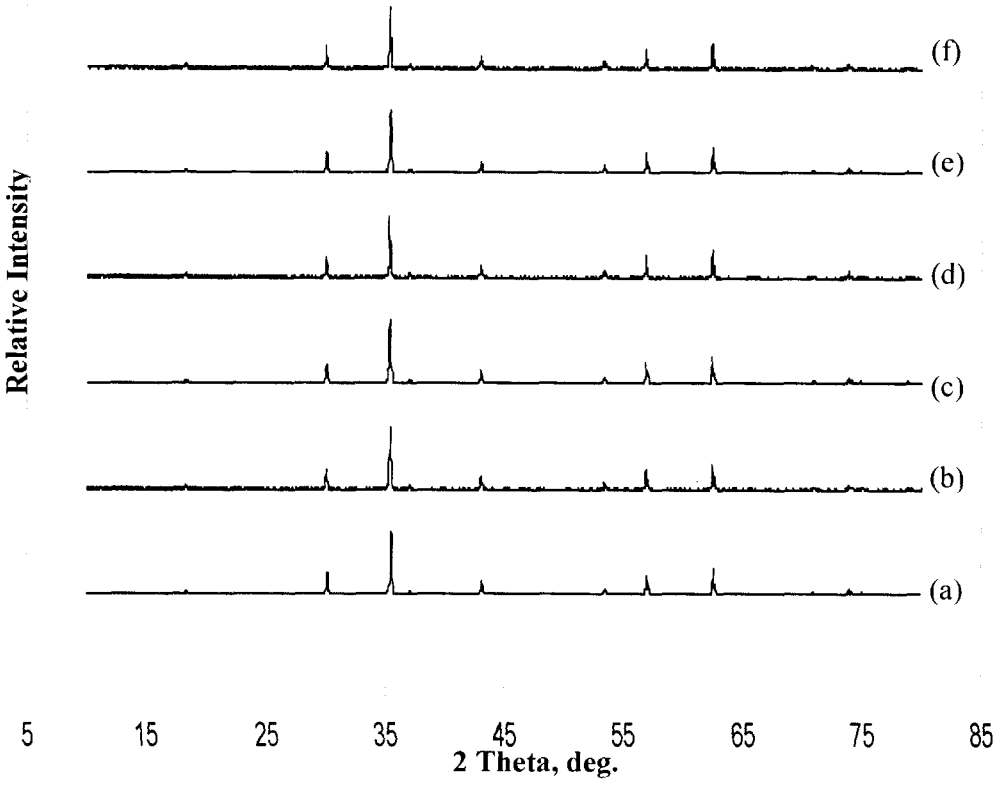

Fig. 4.2.7: XRD analysis for specimens sintered at 950°C with calcination temperature of (a) 650°C, (b) 700°C, (c) 750°C, (d) 800°C, (e) 850°C and (f) 900°C

XRD patterns for specimens sintered at 900°C and 950°C with different calcination temperatures are shown in Fig. 4.2.6 and Fig. 4.2.7, respectively. The XRD spectra show after sintering that complete formation of single spinel phase structure is observed with high sharpness of the major peak and highly narrowing of diffraction line, while no extra peak or secondary phases (especially hematite) are detected. According to Shi et al. [61], the narrowing of diffraction line and high sharpness is probably due to the better order structure or the increase of grain size.

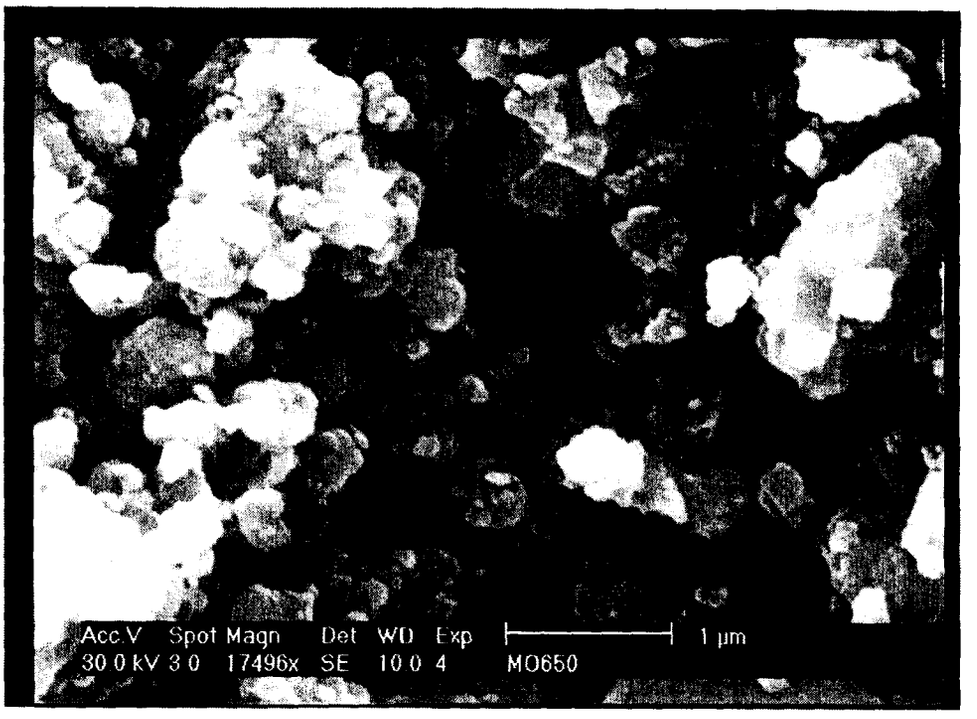

Fig. 4.2.8: SEM micrograph for mixed oxide powder calcined at 650°C

SEM micrographs show the morphological features of the mixed oxide powder calcined at 650°C (Fig. 4.2.8). Fine particles are observed with a milled size less than 1 µm and a tendency to form agglomerates.

Fig. 4.2.9 shows the SEM micrograph of the fracture surface of specimens calcined at 750°C and sintered at 900°C. While Fig. 4.2.10 shows the SEM micrograph of the fracture surfaces of a specimen calcined at 850°C and sintered at 950°C. Between Fig. 4.2.9 and Fig. 4.2.10, the specimen with the higher sintering temperature shows a higher degree of densification because of the higher sinterability observed. As the sintering temperature is increased, the number of pores is decreased due to the increased densification. Furthermore, the specimen with the sintering temperature of 950°C (Fig. 4.2.10) has a grain size larger than the specimen with the sintering temperature of 900°C (Fig. 4.2.9).

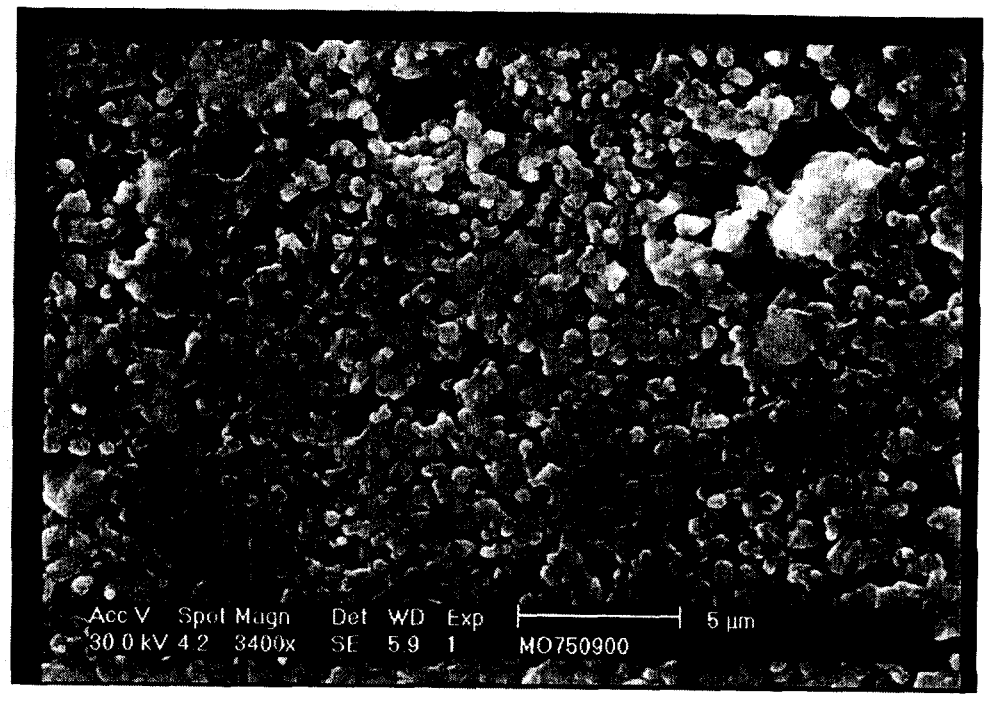

Fig. 4.2.9: SEM micrograph of the fracture surface of a specimen calcined at 750°C and sintered at 900°C

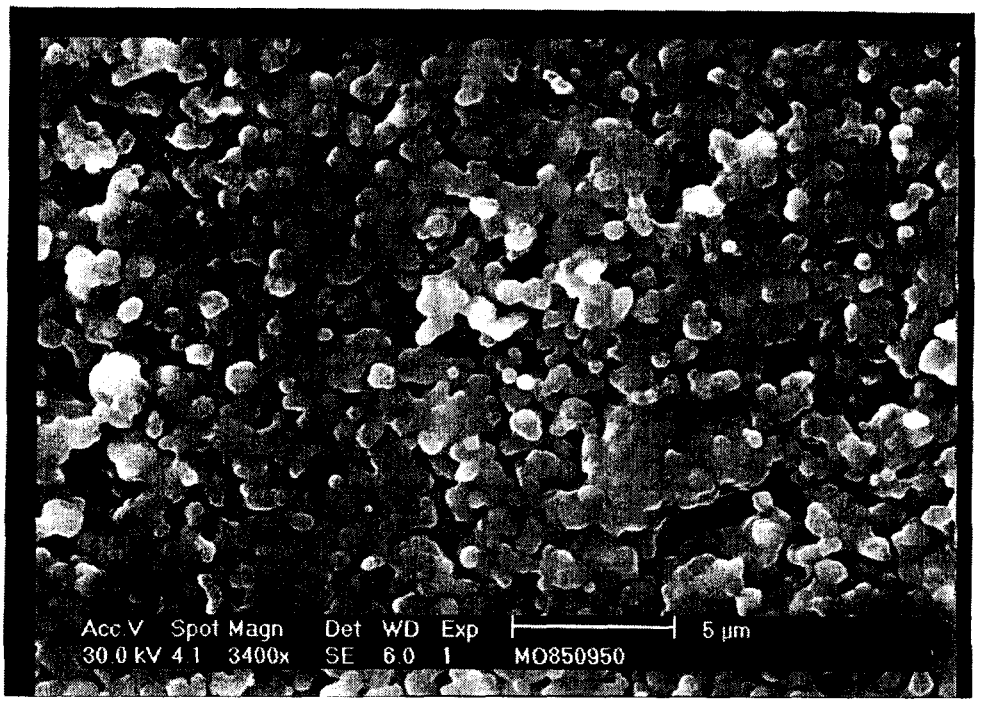

Fig. 4.2.10: SEM micrograph of the fracture surface of a specimen calcined at 850°C and sintered at 950°C

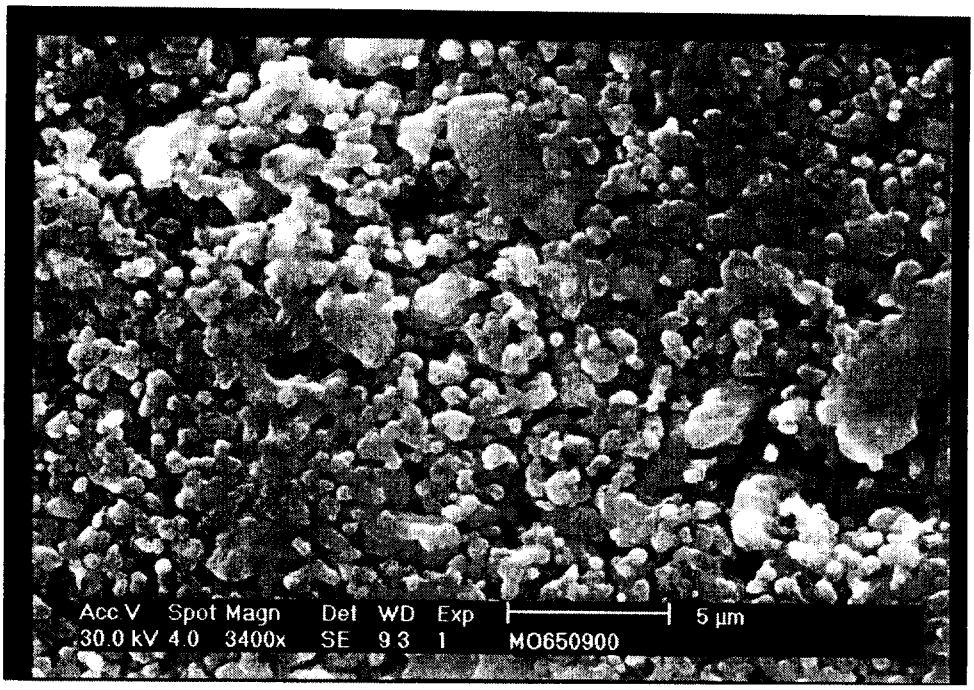

Fig. 4.2.11: SEM micrograph of the fracture surface of a specimen calcined at 650°C and sintered at 900°C

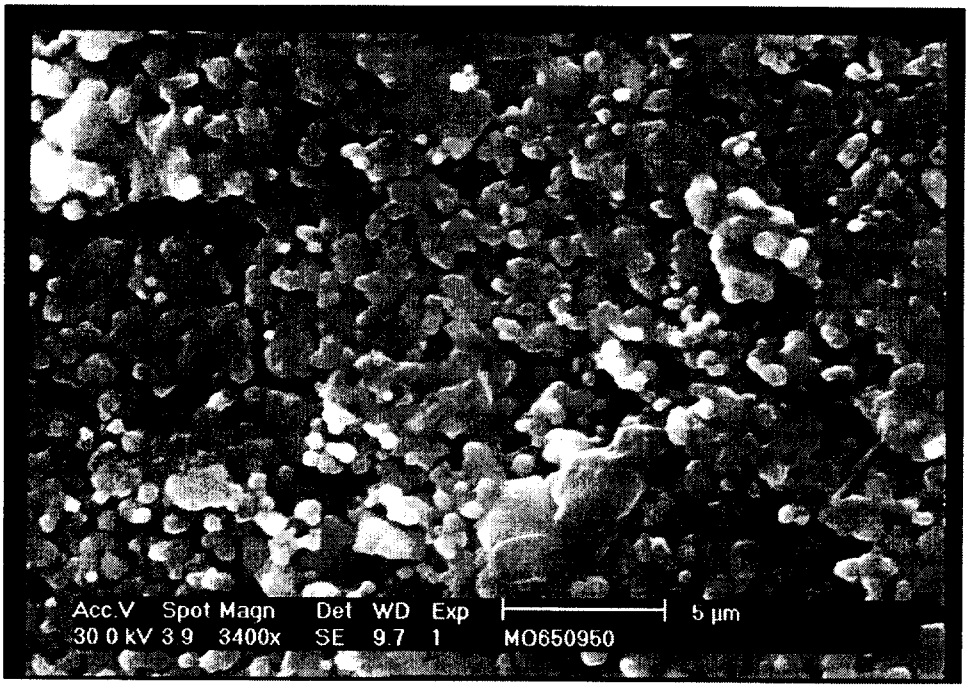

Fig. 4.2.12: SEM micrograph of the fracture surface of a specimen calcined at 650°C and sintered at 950°C

Thus, the grains of ferrite grew as the sintering temperature increased. However, the grain size is difficult to determine and the distribution was comparatively inhomogeneous because non – uniform distribution of pores and grain size can be observed with some agglomerated grains.

Therefore, a higher density can be expected from the specimens with a sintering temperature of 950°C as compared to the specimens with a sintering temperature of 900°C.

The SEM micrograph for specimens calcined at 650°C with sintering temperature of 900°C (Fig. 4.2.11) and 950°C (4.2.12) also shows that specimens with higher sintering temperature posses better densification with a lower amount of porosity.

The milled size of the powders calcined at 650°C and 850°C are shown in Fig. 4.2.13 and 4.2.14, respectively. There are two peaks are observed in Fig. 4.2.13 and 4.2.14. The milled size distribution for first peak generally between 0.1 to 1.0 μm, while the milled size for second small peak between 5.0 to 50 μm. It can be considered that the large particles (between 5.0 to 50μm) are agglomerates of the fine particles that were not perfectly dispersed when the calcined powder was ball milled. Therefore, if only the particles whose granularities are small are considered, the particle size is less than 0.33 μm. This result is also confirmed by SEM micrograph (Fig. 4.2.8) where analysis shows that the milled size is less than 1 μm.

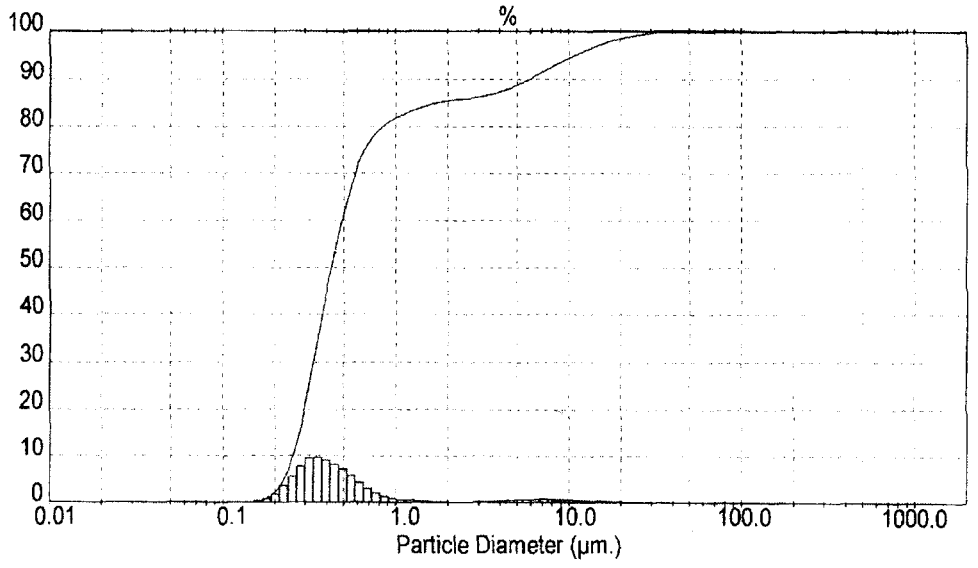

Fig. 4.2.13: Particle size distribution of the powder calcined at 650°C

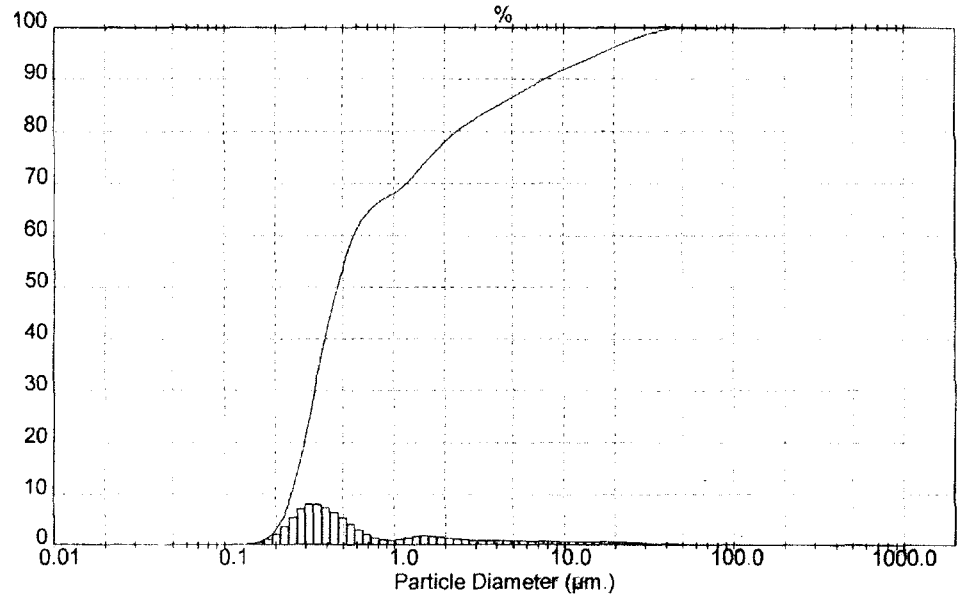

Fig. 4.2.14: Particle size distribution of the powder calcined at 850°C

Densification and Electromagnetic Measurements

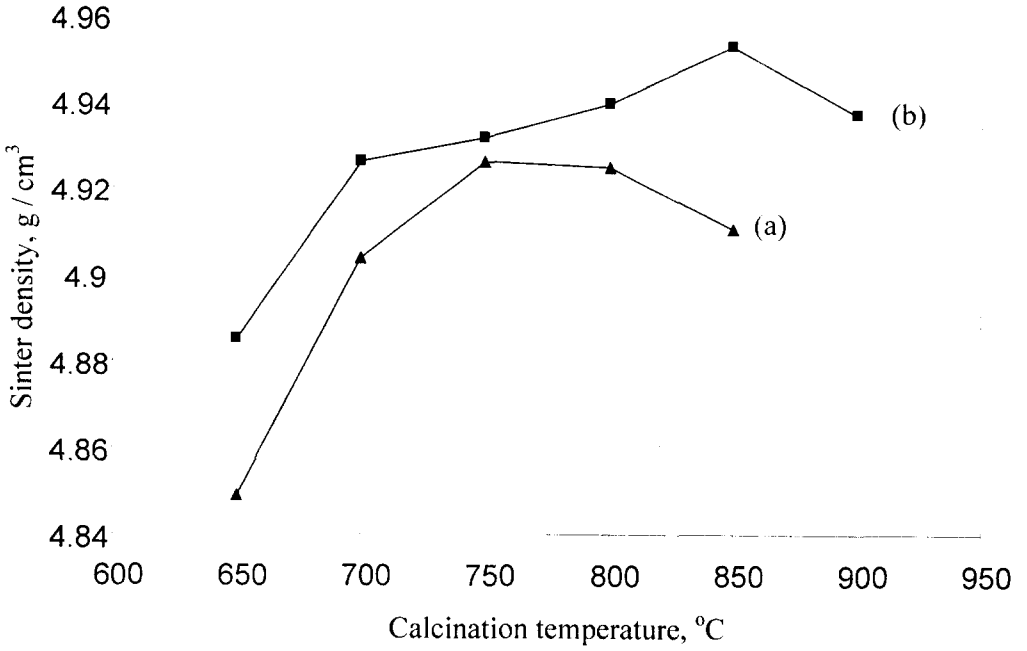

Fig. 4.2.15: Density measurement for specimens with different calcination temperatures and a sintering temperature of (a) 900°C and (b) 950°C

Fig. 4.2.15 shows the variation of the sintered density of MgCuZn ferrites with different calcination and sintering temperature. It shows that both specimens sintered at 900°C and 950°C have an optimum sintered density and lowest percent of porosity (Fig. 4.2.16) at different calcination temperature.

For specimens sintered at 900°C, the sintered density increases with calcination temperature from 650°C until 750°C and then started to drop. For specimens sinter at 950°C, the sintered density increases with calcination temperature from 650°C until 850°C and then started to decrease.

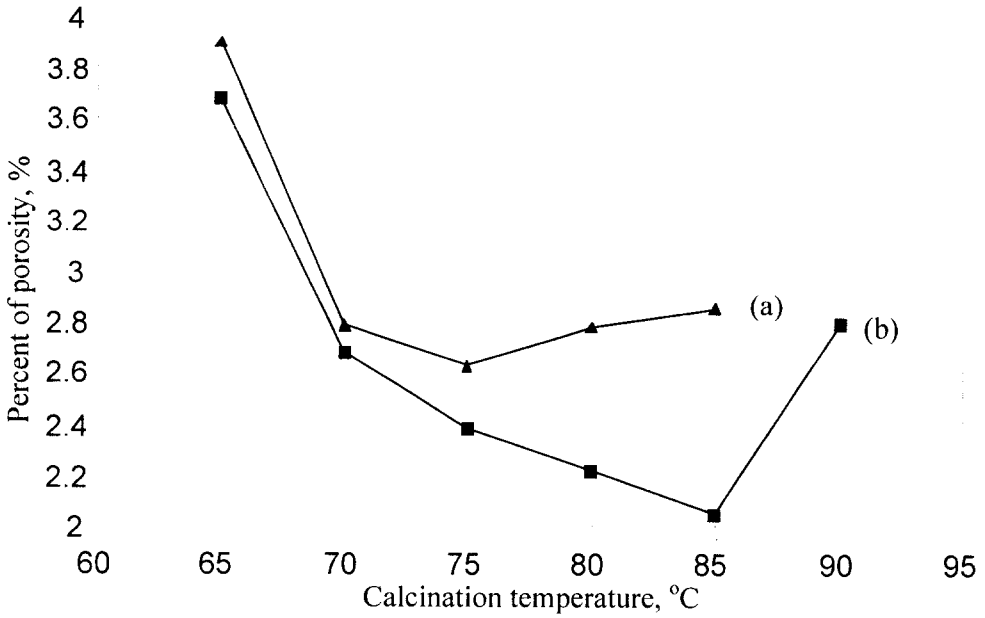

Fig. 4.2.16: Porosity measurement for specimens with different calcination temperatures and a sintering temperature of (a) 900°C and (b) 950°C

According to Nakahata et al. [22] and Murthy [20], a different calcination temperature requires a different sintering temperature to achieve a particular amount of shrinkage during sintering. Therefore, densification is not only affected by the sintering temperature but also by the calcination temperature because a different surface area will be produced.

It can be observed that the specimen calcined at 850°C and sintered at 950°C produces a higher density (4.9529 g / cm^3) as compared to the specimens calcined at 750°C and sintered at 900°C (4.9262 g / cm^3). This result is confirmed by SEM microstructure (Fig. 4.2.9 and 4.2.10), which shows that the fracture surface of the specimen sintered at 950°C is denser and less porous than the one sintered at 900°C. Overall the porosity for all calcined and sintered specimens is between 2 to 4% (Fig. 4.2.16). However, SEM microstructure (Fig. 4.2.9 and 4.2.10) shows that big pores are observed. Since pores are divided into open pores and closed pores, while the

fracture surface (SEM microstructure) mainly showed the open pores, therefore, the percent of porosity that observed is suspected to be referred to the closed pores.

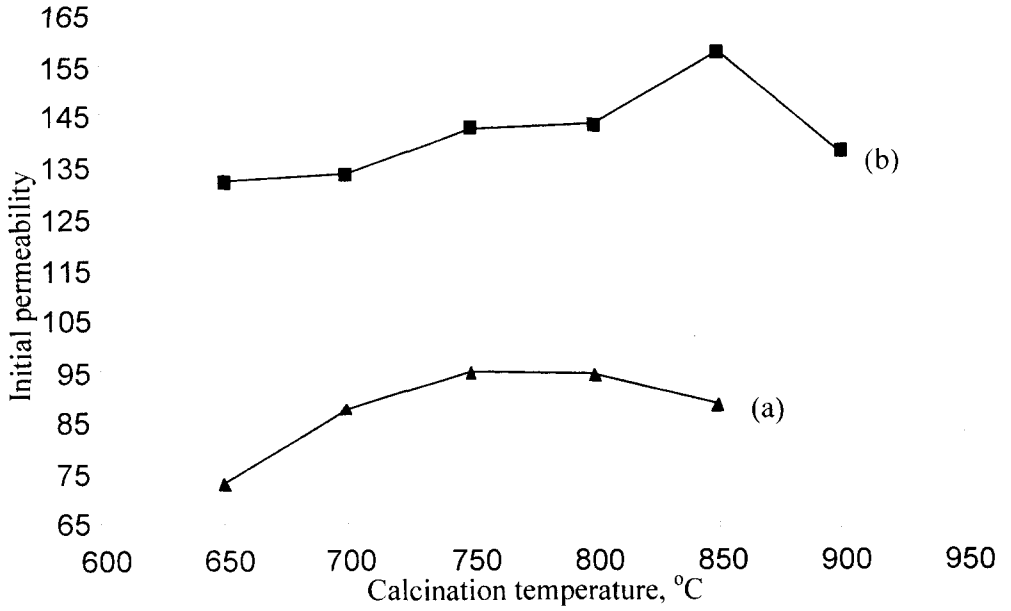

Fig. 4.2.17: Initial permeability (at 100 kHz) for specimens with different calcination temperatures and a sintering temperature of (a) 900°C and (b) 950°C

Fig. 4.2.17 show the initial permeability as a function of calcination temperature for specimens sintered at 900°C and 950°C. It is clearly seen that the initial permeability for specimens sintered at 900°C increases up to a calcination temperature of 750°C, then, the initial permeability started to deteriorate as the calcination temperature exceeded 750°C. For specimens sintered at 950°C, it can be observed that the initial permeability increases until a calcination temperature of 850°C and then started to decrease.

It is known that initial permeability is greatly affected by grain size, porosity, chemical composition and the presence of second phases [64]. Since there are no differences in chemical composition, the initial permeability may be expected to be influenced by grain size, porosity, density and the presence of secondary phases.

From SEM microstructure (Fig. 4.2.9 and 4.2.10), as the sintering temperature is increased, the grain size and the sintered density (Fig. 4.2.15) are increased. According to Goldman [33], an increase in grain size will cause an increase in initial permeability. Fig. 4.2.17 shows the same trend as mentioned by Goldman. Therefore, the initial permeability is expected to increase with increasing grain size and sintered density.

The presence of porosity will also affect the initial permeability. Fig. 4.2.16 shows that an increase in porosity will cause a reduction in initial permeability (Fig. 4.2.17). The presence of porosity could effectively pin the domain wall movement and cause a reduction in initial permeability. Thus, by removal of domain wall pinning sites through the increase in grain size and improvement of densification, the grain boundary area will decrease, causing an increase in initial permeability.

At calcination temperature lower than 900°C a secondary phase of hematite (α - Fe_2O_3) is detected in MgCuZn ferrites (Fig. 4.2.5). As the calcination temperature increases, the hematite phase is gradually reduced until undetected at 900°C. Previously, it was considered that the presence of second phases will affect the initial permeability. However, Fig. 4.2.17 indicates that the initial permeability is not affected by the presence of hematite phase but greatly influenced by grain size and densification behaviour. Furthermore, the optimum value of initial permeability is found at a calcination temperature higher than 750°C. Therefore, it is believed that by improving the ferrite formation at higher calcination temperatures, the crystallinity is increased, causing the increase in initial permeability.

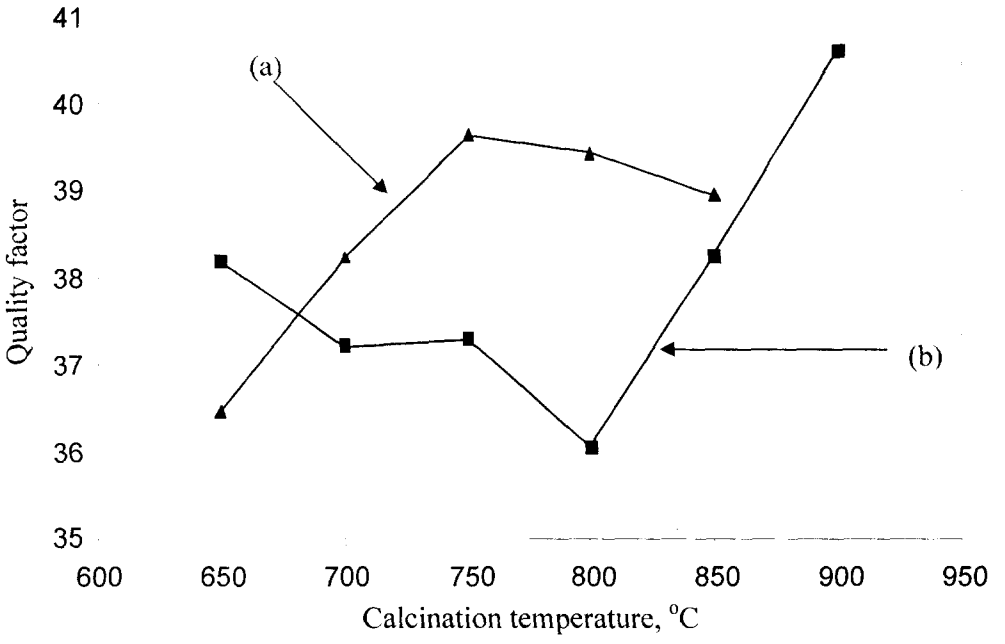

Fig. 4.2.18: Quality factor (at 100 kHz) for specimens with different calcination temperatures and a sintering temperature of (a) 900°C and (b) 950°C

Fig. 4.2.18 shows the quality factor as a function of calcination temperature for specimens sintered at 900°C and 950°C at frequency of 100 kHz. It is clearly seen that the quality factor for specimens sintered at 900°C follow the trend found for the initial permeability (Fig. 4.2.17), which is believed to be affected by grain size, density, chemical composition and the presence of secondary phases. However, the trend of quality factor for specimens sintered at 950°C is opposite to the trend show in Fig. 4.2.17, but almost similar to the trend of DC electrical resistivity (Fig. 4.2.19), which will be discussed later.

For specimens sintered at 950°C, the specimens with a calcination temperature less than 650°C or more than 900°C have quality factor higher than specimens sinter at 900°C. However, for specimens with a calcination temperature between 700°C and 850°C, the specimens with a sintering temperature of 900°C have a higher quality factor than the specimens sintered at 950°C.

According to Nakano et al. [78], the quality factor of ferrites is strongly affected by impurities. Furthermore, Nakano et al. thought that the resistivity of ferrite materials is closely related to the quality factor. It is believed that a higher quality factor is due to the high resistivity of the material. This is confirmed by comparing Fig. 4.2.18 and Fig. 4.2.19. From Fig. 4.2.18, the trend of specimens sinter at 950°C is decreased from calcination temperature of 650°C to 800°C and then increased. This trend is similar to the trend of DC electrical resistivity (Fig. 4.2.19).

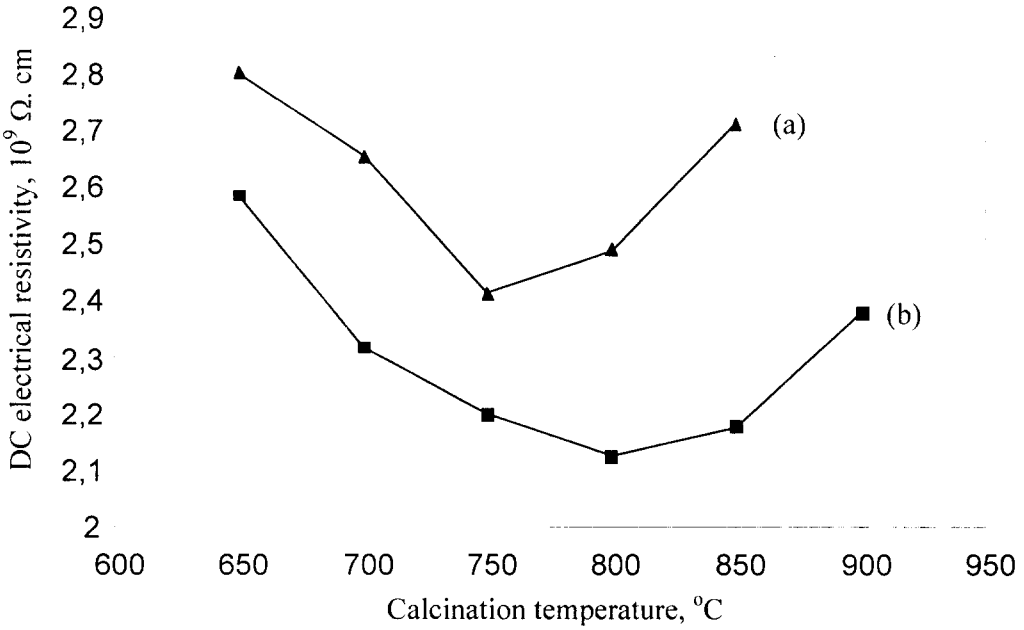

Fig. 4.2.19: DC electrical resistivity measurement for specimens with different calcination temperatures and a sintering temperature of (a) 900°C and (b) 950°C

The variation of the DC electrical resistivity with calcination and sintering temperature is illustrated in Fig. 4.2.19. For specimens sintered at 900°C, as calcination temperature is increased, the DC electrical resistivity will reduce and reach a minimum level at 750°C and then the DC electrical resistivity increase. For specimens sinter at 950°C, the same trend is observed as the DC electrical resistivity will be reduced and reach a minimum level at 800°C and then the DC electrical

resistivity increases. Fig. 4.2.19 also indicates that specimens with a higher sintering temperature show a lower resistivity value.

In combination with Fig. 4.2.16 (percent of porosity) and Fig 4.2.19, a material with a higher amount of porosity has a higher DC electrical resistivity value. When the porosity is increased, the number of pores, vacancies and scattering centres for the electrical charge carriers will be increased, which will lead to an increase in DC electrical resistivity. The porosity actually act as barriers to the flow of electrons.

Resistivity of ferrites is increased with a decrease in grain size [47]. Ferrites of smaller grain size have a larger grain boundary area, which will act as barriers to the electron movement and trap imperfections, such as porosity, impurities and etc. SEM microstructure (Fig. 4.2.9 and 4.2.10) shows that at higher sintering temperature, the grain size is larger with less porosity. As compared to SEM microstructure, the larger the grain size, the lower the DC electrical resistivity (Fig. 4.2.19).

Therefore, DC electrical resistivity may be expected to be influenced by grain size, porosity, calcination temperature and sintering temperature.

The loss factor (Fig. 4.2.20) is important for multilayer chip inductors. In general, the loss factors obtained are in the order of 10^{-4}. The loss factor indicates the magnetic losses, which are divided into hysteresis loss, eddy–current loss and residual loss. The lower the loss factor, the better the ferrite is.

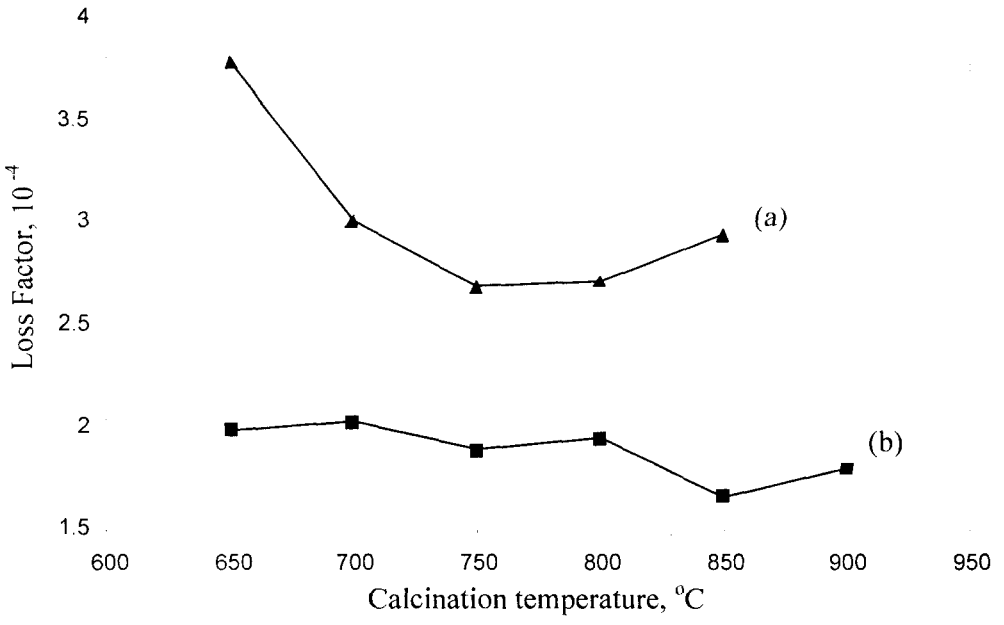

Fig. 4.2.20: Loss factor measurement for specimens with different calcination temperatures and a sintering temperature of (a) 900°C and (b) 950°C

The frequency used in this research is 100 kHz. When the frequency that is used is lower than 500 kHz, the residual loss can be ignored [67]. The eddy – current loss is reciprocal to the resistivity and proportional to the square of the frequency. Since the resistivity value obtained is high, in the order of 10^9, the eddy – current loss is considered to be negligible. Thus, the total magnetic losses are considered to be predominantly hysteresis loss. The hysteresis loss is sensitive to microstructural homogeneity and to the presence of secondary phases. Therefore, any increase of the porosity content will increase losses.

From Fig. 4.2.20, different sintering temperature will result in different loss factor. For specimens sinter at 900°C, a calcination temperature of 750°C will give the minimum loss factor. For specimens with a sintering temperature of 950°C, minimum loss factor is found at a calcination temperature of 850°C. However, the dependence of calcination temperature to loss factor for specimens sintered at 950°C

is weak. The decrease in loss factor may be due to the decrease of domain wall pinning and grain boundaries. Thus, the reduction in losses might be due to the reduction in porosity.

The specimens prepared from powder with a calcination temperature of 850°C and sintering temperature of 950°C shows the absent of second phases (hematite), highest density, lowest porosity, highest initial permeability, good quality factor, good DC electrical resistivity and lowest loss factor value.

However, it can be observed that a higher sintering temperature will required a higher calcination temperature, in order to achieve optimum properties. Therefore, in the next section, calcination temperatures of 800°C and 850°C are selected for the investigation of optimum sintering temperature by mixed oxide route.

4.2.2 The Investigation of Optimum Sintering Temperature Characterization of MgCuZn Ferrites

The SEM microstructure of fracture surface are shown for a specimen calcined at 750°C with a sintering temperature of 900°C (Fig. 4.2.21), a specimen calcined at 800°C with a sintering temperature of 930°C (Fig. 4.2.22), a specimen calcined at 850°C with a sintering temperature of 930°C (Fig. 4.2.23) and a specimen calcined at 850°C with a sintering temperature of 950°C (Fig. 4.2.24).

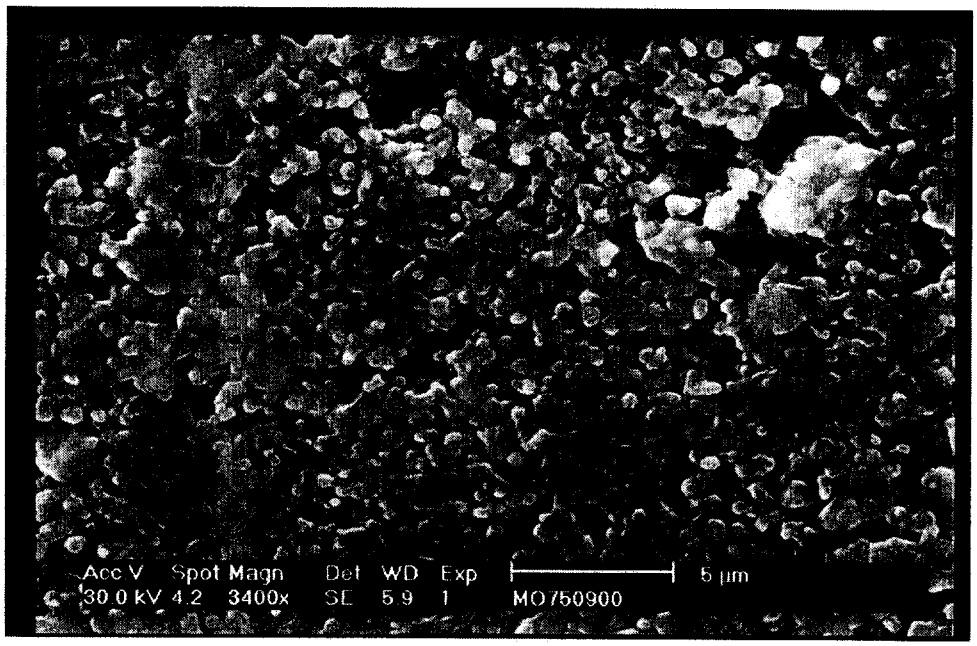

Fig. 4.2.21: SEM micrograph of the fracture surface of a specimen calcined at 750°C and sintered at 900°C

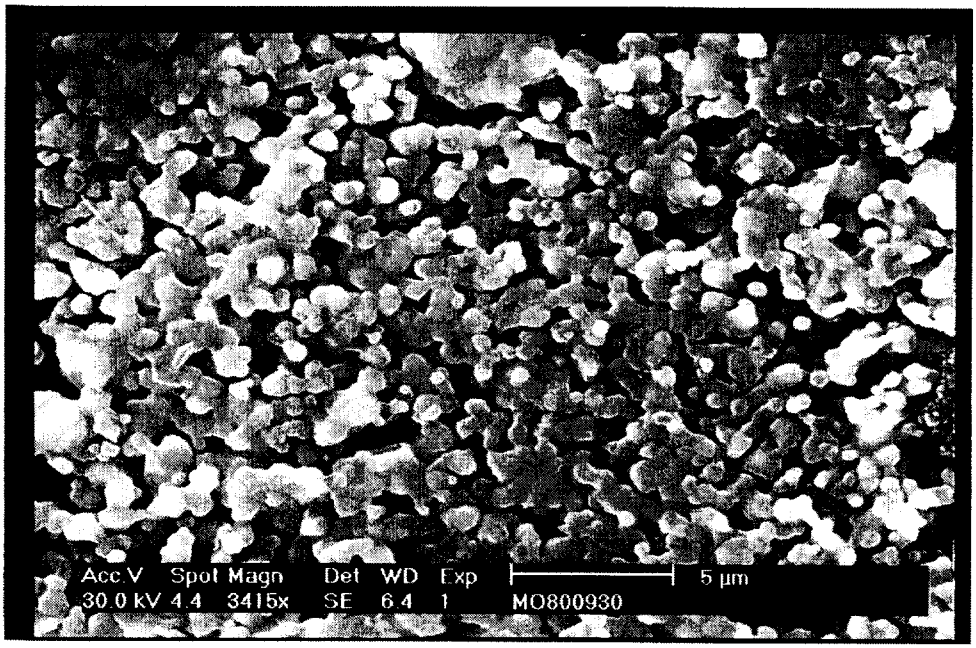

Fig. 4.2.22: SEM micrograph of the fracture surface of a specimen calcined at 800°C and sintered at 930°C

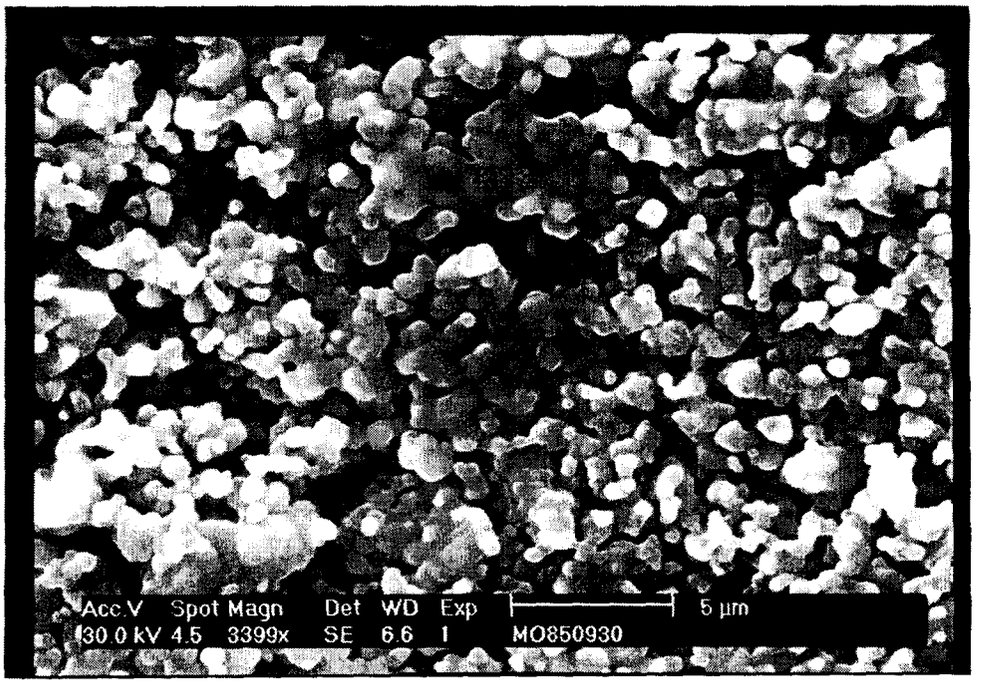

Fig. 4.2.23: SEM micrograph of the fracture surface of a specimen calcined at 850°C and sintered at 930°C

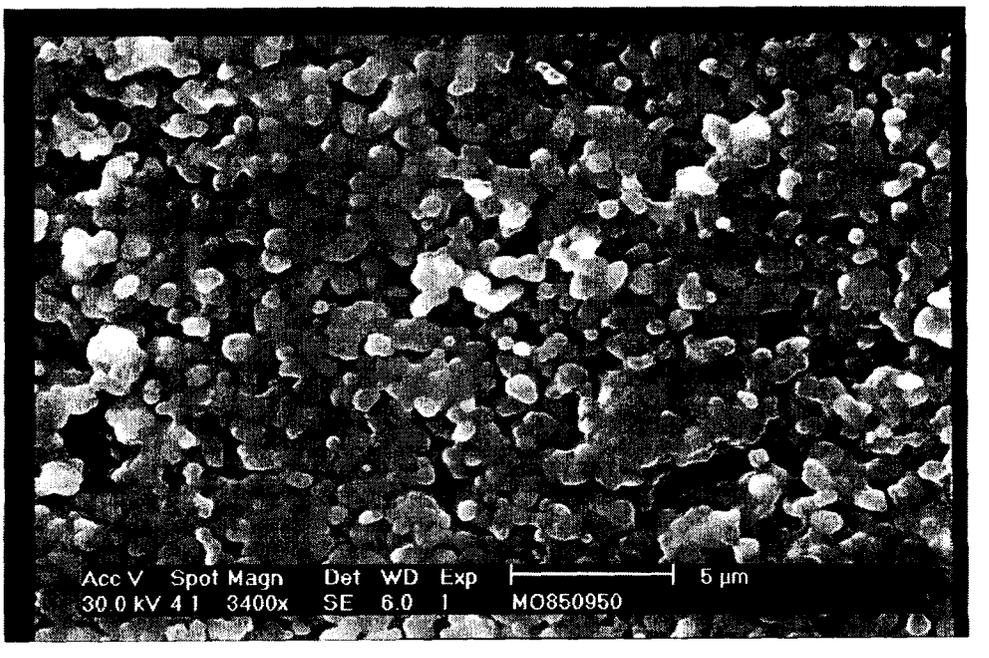

Fig. 4.2.24: SEM micrograph of the fracture surface of a specimen calcined at 850°C and sintered at 950°C

Overall, SEM microstructure reveals that the specimen with a calcination temperature of 750°C and sintering temperature of 900°C (Fig. 4.2.21) consists of smaller grains than the others (Fig. 4.2.22, 4.2.23 and 4.2.24). Furthermore, SEM microstructure reveals that the specimens with a calcination temperature of 850°C and a sintering temperature of 950°C (Fig. 4.2.24) shows a higher degree of densification with higher sinterability and lower porosity than the others (Fig. 4.2.21, 4.2.22 and 4.2.23). Therefore, as the sintering temperature is increased, the grain size is increased together with an improvement in densification.

In general, the grain size of all the specimens is smaller than 2 μm. However, the actual grain size is still difficult to determine due to inhomogeneous distribution of grain size together with non–uniform distribution of pores and some agglomeration.

Densification and Electromagnetic Measurements

In this section, four types of sintered MgCuZn ferrites were selected according to the method of processing as follows:

a) Mixed oxide route with the specimens calcined at 800°C and sintered at 900°C (MO 800-900).

b) Mixed oxide route with the specimens calcined at 800°C and sintered at 930°C (MO 800-930).

c) Mixed oxide route with the specimens calcined at 850°C and sintered at 930°C (MO 850-930).

d) Mixed oxide route with the specimens calcined at 850°C and sintered at 950°C (MO 850-950).

Table 4.2.1: Density and porosity measurement for specimens with different calcination temperature and a sintering temperature of 900°C, 930°C and 950°C

Calcination temperature, °C - sintering temperature, °C	Sinter density, g / cm^3		Porosity, %
	Theoretical	sintered	
800 - 900	5.065	4.9246	2.772
800 - 930	5.0659	4.9267	2.7478
850 - 930	5.061	4.9366	2.458
850 - 950	5.0563	4.9529	2.045

The sinter density and porosity measurement of sintered MgCuZn ferrites with sintering temperature of 900°C, 930°C and 950°C using mixed oxide route are shown in Table 4.2.

Generally, the sintered density is increased from a sintering temperature of 900°C to 950°C. Overall, MgCuZn ferrites produced by mixed oxide route have a sintered density higher than 95% of the theoretical density calculated from the XRD results.

It can be observed that the porosity for specimens calcined at 850°C and sintered at 950°C is the lowest. This observation is confirmed by SEM microstructure (Fig. 4.2.21, 4.2.22, 4.2.23 and 4.2.24), where specimens with a sintering temperature of 950°C show a higher degree of densification and lower porosity than others.

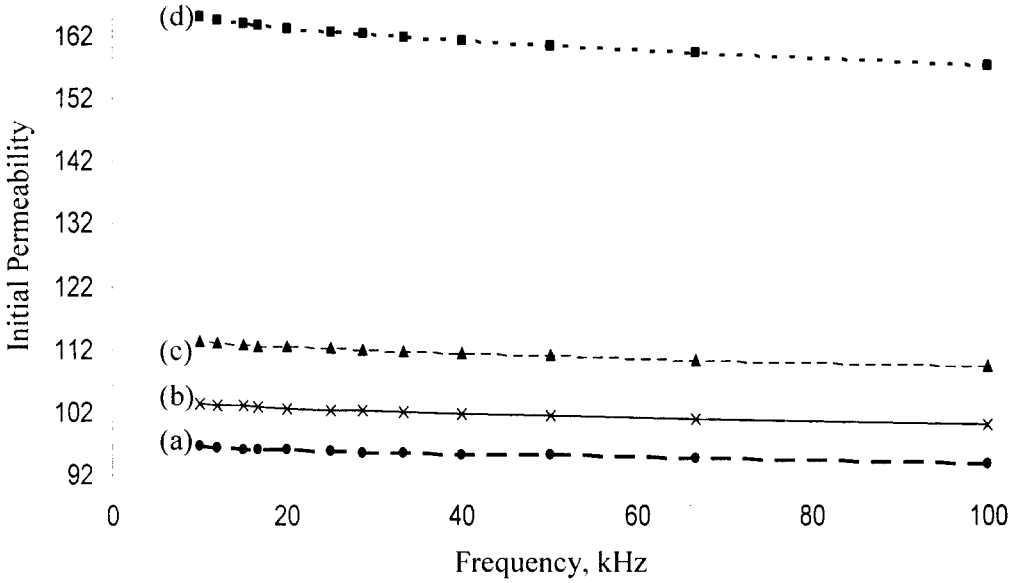

Fig. 4.2.25: Initial permeability measurement for specimens (a) calcined at 800°C and sintered at 900°C (b) calcined at 800°C and sintered at 930°C (c) calcined at 850°C and sintered at 930°C and (d) calcined at 850°C and sintered at 950°C

Fig. 4.2.25 shows the initial permeability versus frequency for specimens with a sintering temperature of 900°C, 930°C and 950°C, respectively. It can be seen that the initial permeability of the specimens is increased from a sintering temperature of 900°C to 950°C and specimens calcined at 850°C and sintered at 950°C posses the highest initial permeability. Overall, slight reduction in initial permeability is observed from low to high frequency.

The initial permeability (at frequency between 10 to 100 kHz) of the specimens calcined at 800°C and sintered at 900°C was 93 to 96, specimens calcined at 800°C and sintered at 930°C range from 100 to 103, specimens calcined at 850°C and sintered at 930°C from 109 to 113 and specimens calcined at 850°C and sintered at 950°C from 157 to 165.

Overall, the increase in initial permeability with sintering temperature is due to the increase in grain size (Fig. 4.2.21 to 4.2.24), increase in sintered density and the reduction in porosity (Table 4.2). As sintering temperature is increased, the grain size is increased, reducing the grain boundary area, which results in the removal of domain wall pinning sites. Therefore, initial permeability is expected to increase and the observations are matched with these factors.

It can be observed from Fig. 4.2.26 that the quality factor increases with frequency from 10 kHz to 100 kHz. This characteristic is different as compared to initial permeability. For initial permeability, a slight reduction in initial permeability is observed from low to high frequency, while for the quality factor, the value increases from low to high frequency.

It also can be seen that specimens with a calcination temperature of 800°C and sintering temperature of 900°C behave differently according to frequency. At frequency lower than 40 kHz, the quality factor value is the lowest as compared to other specimens. However, at frequencies higher than 65 kHz, the quality factor value for this specimen is higher than other specimens. Overall, the quality factor value (from frequency of 10 to 100 kHz) for this specimen is increased from 6 to 39. Generally, the quality factor (Q) of a magnetic component is defined by the following equation [33]:

$$Q = (2 \pi f L) / R_S \quad \text{(4.2.1)}$$

Where, f is frequency, L is inductance and R_S is series resistance (ohms).

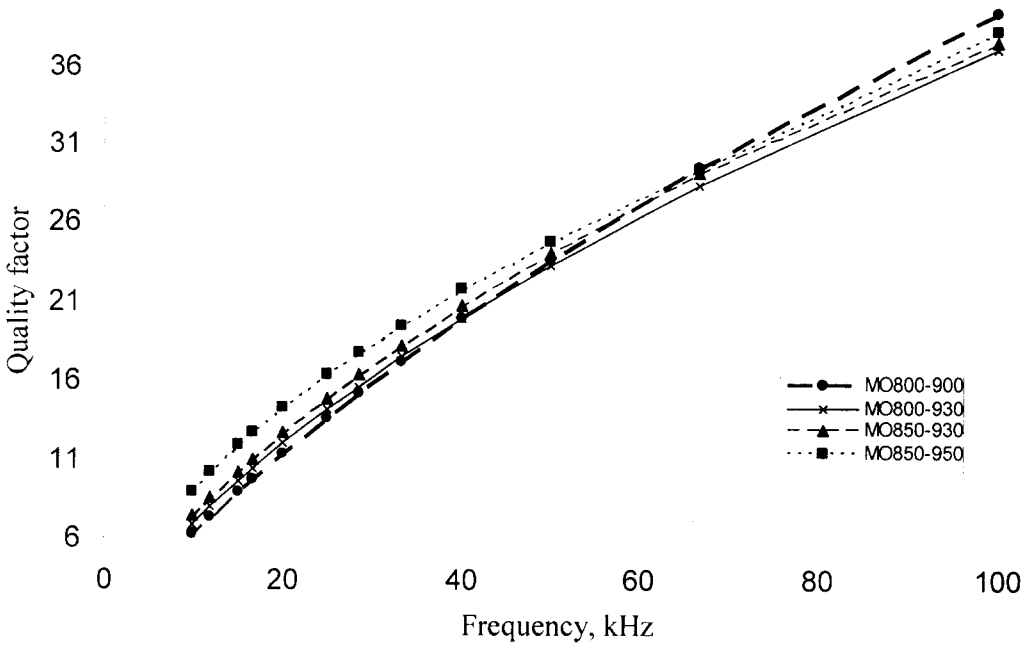

Fig. 4.2.26: Quality factor measurement for specimens calcined at 800°C and sintered at 900°C, specimens calcined at 800°C and sintered at 930°C, specimens calcined at 850°C and sintered at 930°C and specimens calcined at 850°C and sintered at 950°C

Since the initial permeability is proportional to the inductance and Fig. 4.2.25 shows a constant result in initial permeability value, where the specimen with a calcination temperature of 800°C and a sintering temperature of 900°C shows the lowest initial permeability as compared to the other specimens throughout the frequency range between 10 to 100 kHz, therefore, it may be expected that $\mathbf{R_S}$ will influence the quality factor value of this specimen. The increase in frequency may cause a reduction in $\boldsymbol{R_S}$. Thus, the higher the frequency, the better this specimen is because the losses (especially eddy–current losses) are lower through the reduction in $\boldsymbol{R_S}$ value.

Apart from the specimen with a calcination temperature of 800°C and a sintering temperature of 900°C, it appears that the quality factor of the other specimens

increases with sintering temperature. It also reveals that the increase in quality factor is due to the increase in sintered density and grain size. The quality factor (for frequency of 10 to 100 kHz) of the specimen with a sintering temperature of 930°C increased from 6 to 37, whereas for specimen with sintering temperature of 950, the quality factor is increased from 8 to 38. The trend of quality factor of these specimens is similar to that found for initial permeability because by increasing the sintering temperature, the initial permeability and quality factor are increased, which is expected to be due to the increased in grain size, better densification and lower porosity.

Fig. 4.2.27 shows the effect of frequency and sintering temperature on the AC electrical resistivity of MgCuZn ferrite measured at room temperature. All the specimens show a trend of reduction from frequency of 10 kHz to 100 kHz. Overall, all specimens show different AC electrical resistivity at particular frequency.

The resistive grain boundaries were found to be more effective at lower frequencies while the conductive ferrites grains are more effective at higher frequencies [68]. This observation is confirmed by Fig. 4.2.27, where the AC resistivity decreases as the frequency is increased. These grain boundaries were formed by the superficial reduction or oxidation of the crystallites in the porous material as a result of their direct contact with firing atmosphere [72].

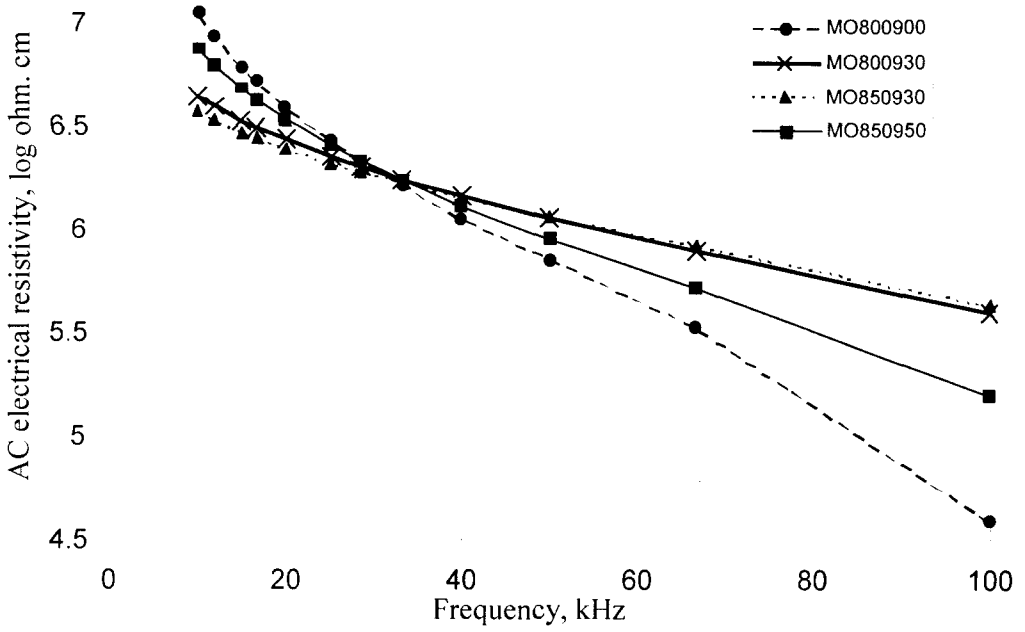

Fig. 4.2.27: AC electrical resistivity measurement for specimens calcined at 800°C and sintered at 900°C, specimens calcined at 800°C and sintered at 930°C, specimens calcined at 850°C and sintered at 930°C and specimens calcined at 850°C and sintered at 950°C

From Fig. 4.2.27, it can be observed that all specimens have the same AC electrical resistivity value at about 30 kHz. Below the frequency of 30 kHz, the AC electrical resistivity of specimens with calcinations temperature of 800°C and sintered at 900°C is higher than other specimens. It is suspected that the resistive grain boundary effect of the specimens is more pronounce than other specimens. However, above the frequency of 30 kHz, the AC electrical resistivity of specimens calcined at 800°C and sintered at 900°C is lower than other specimens. It is suspected that the conductive ferrite grains of these specimens are more pronounce than other specimens.

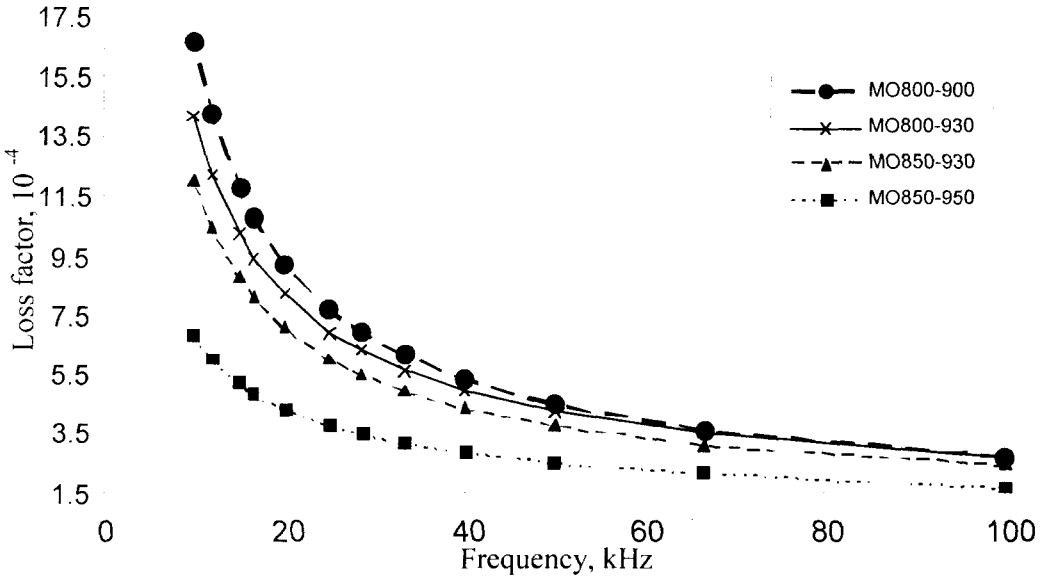

Fig. 4.2.28: Loss factor measurement for specimens calcined at 800°C and sintered at 900°C, specimens calcined at 800°C and sintered at 930°C, specimens calcined at 850°C and sintered at 930°C and specimens calcined at 850°C and sintered at 950°C

The loss factor is plotted against frequency in Fig. 4.2.28 for MgCuZn ferrites sintered at a temperature of 900°C, 930°C or 950°C. From a frequency of 10 kHz to 100 kHz, the loss factor is observed to decreased and is believed to reach a minimum level as the frequency increases to more than 100 kHz. In general, the loss factor is in the order of 10^{-4}. The specimen with a calcination temperature of 850°C, sintered at 950°C was found to exhibit the lowest loss factor as compared to other specimens. From Fig. 4.2.28 and Table 4.2, it was found that the higher the sintering temperature, the lower the loss factor, coinciding with higher sintered density and lower porosity.

For ferrites to be useful as inductor materials, there should have a high density, low porosity, high initial permeability, high quality factor, high AC electrical resistivity and low loss factor over the frequency range of interest. Thus, specimens calcined at 850°C and sintered at 950°C would be preferred in the mixed oxide route.

4.3 Comparison Between the Properties of the Specimens Prepared by Co-precipitation Process and Mixed Oxide Route

In this section, three types of sintered MgCuZn ferrites were selected according to the method of processing as follows:

a) Co-precipitation process with the specimens dehydrated at 180°C and sintered at 930°C (CP 180-930).

b) Co-precipitation process with the specimens calcined at 650°C and sintered at 930°C (CP 650-930).

c) Mixed oxide route with the specimens calcined at 850°C and sintered at 950°C (MO 850-950).

Each of the above specimens was chosen due to their optimum properties at a particular processing methods.

The above specimens were selected for the purpose of comparison between the properties (densification and electromagnetic properties) of the specimens prepared by co-precipitation process and mixed oxide route.

4.3.1 Characterization of MgCuZn Ferrites

XRD analysis

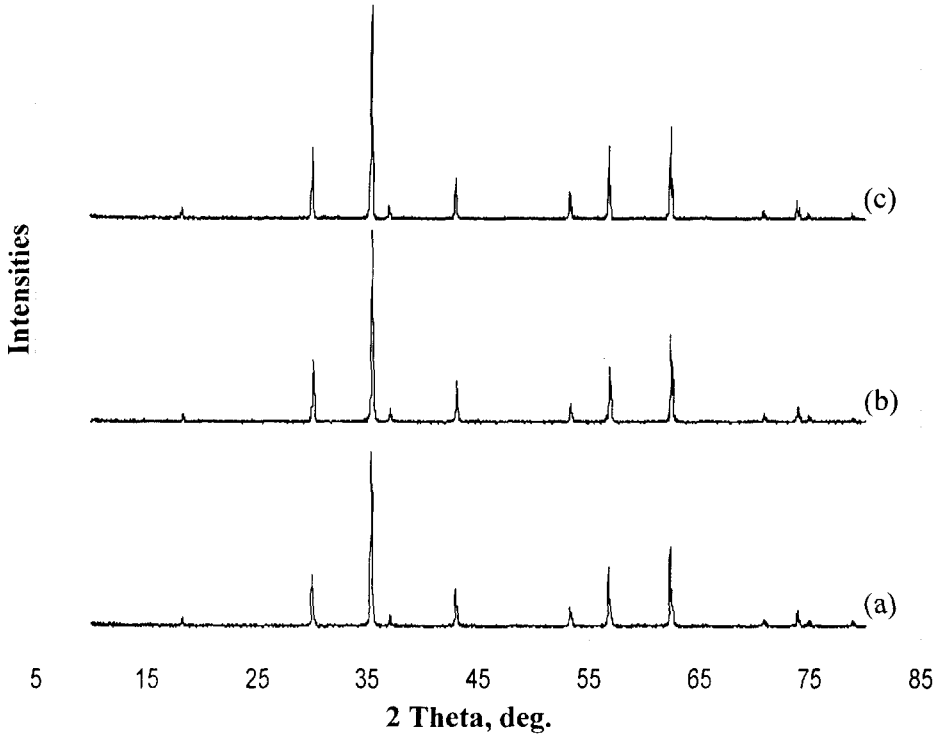

Fig. 4.3.1: XRD analysis for specimens prepared by (a) Co-precipitation process (CP 180 – 930), (b) Co-precipitation and calcined (CP 650 – 930) and (c) Mixed oxide route (MO 850 – 950)

XRD results for the three specimens are shown in Fig. 4.3.1. The results confirmed that all the specimens crystallize in the spinel structure and match well to the characteristics reflections of magnesium ferrite, irrespective of the method of preparation. The peaks at $2\theta \approx 18.2^{\circ}$, 30°, 35.5°, 37°, 43°, 53.5°, 57°, 62.5°, 70.5°, 74.5°, 75° and 79° appeared indicating the formation of a crystallite phase of spinel structure of MgCuZn ferrites.

SEM analysis

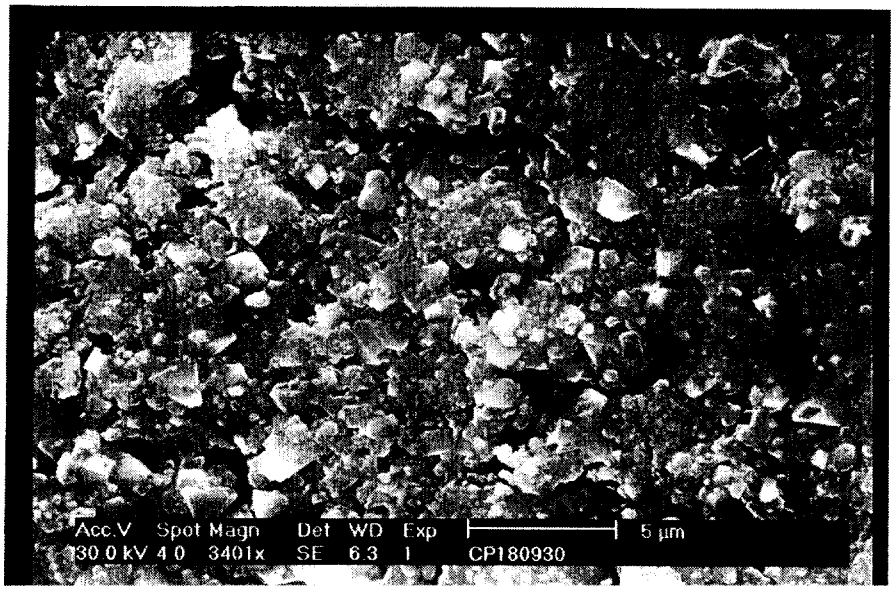

Fig. 4.3.2: SEM micrograph of the fracture surface of a specimen dehydrated at 180°C and sintered at 930°C by co-precipitation process

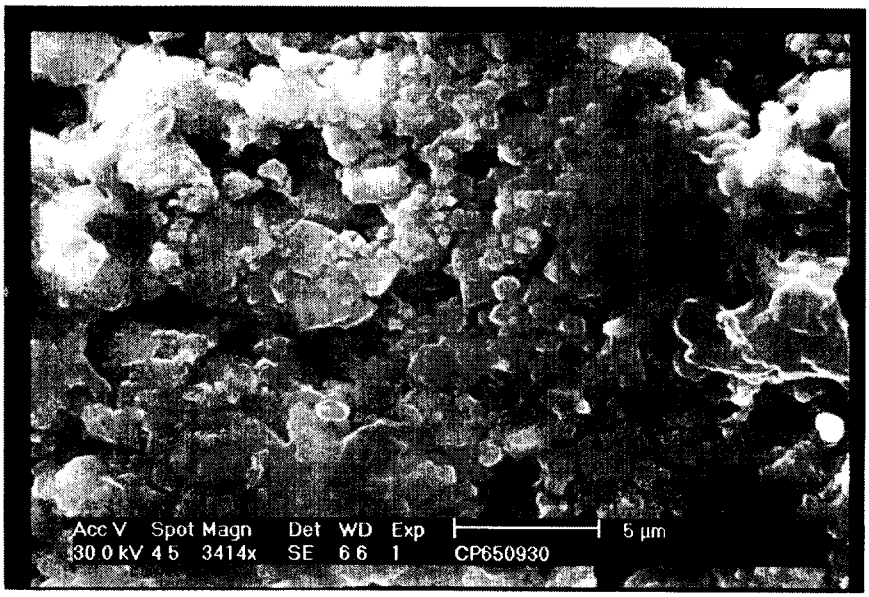

Fig. 4.3.3: SEM micrograph of the fracture surface of a specimen calcined at 650°C and sintered at 930°C by co-precipitation process

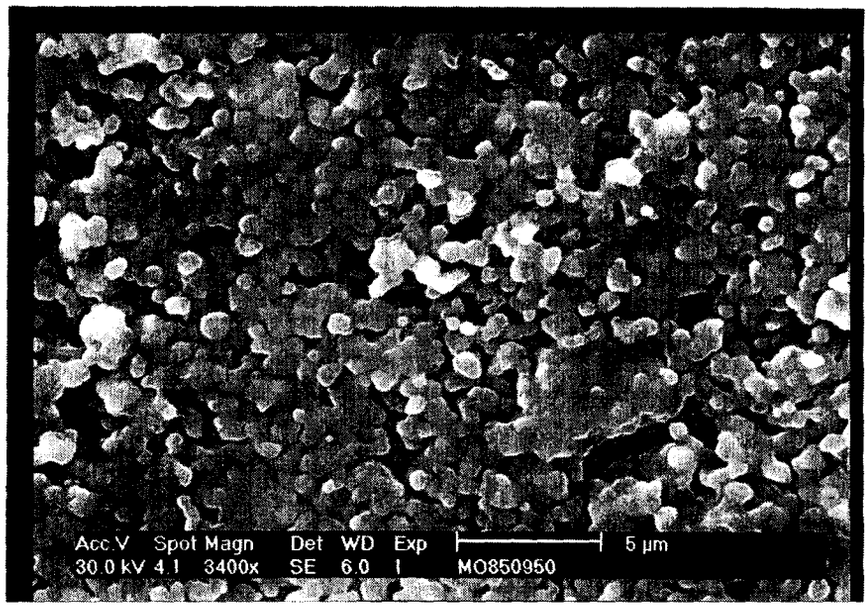

Fig. 4.3.4: SEM micrograph of the fracture surface of a specimen calcined at 850°C and sintered at 950°C by mixed oxide route

Microstructure study on fracture surface of MgCuZn ferrites synthesize by co-precipitation process and mixed oxide route are shown in Fig. 4.3.2, 4.3.3 and 4.3.4. The microstructure was quite different for both co-precipitation and mixed oxide route, which might give a rough idea about sintering and grain size nature. However, the grain size measurement from fracture surface of SEM micrograph was difficult because it was quite hard to locate clear grain / grain boundary interface.

4.3.2 Densification and Electromagnetic Measurements

Table 4.3.1: Densities and porosity measurement of MgCuZn ferrites prepared by co-precipitation process, co-precipitation process and calcined and mixed oxide route

Sample	Sinter density, g / cm^3		Porosity, %
	Theoretical	sinter	
CP 180 - 930	5.065	4.9002	3.2537
CP 650 - 930	5.0664	4.9669	1.9639
MO 850 - 950	5.0563	4.9529	2.045

The densities of sintered MgCuZn ferrites using co-precipitation process and mixed oxide route are shown in Table 4.3. Generally, the sintered densities of co-precipitation and mixed oxide sintered ferrites lie in the same range. However, co-precipitated specimens with dehydrated temperature of 180°C and sintered at 930°C shows the highest amount of porosity.

Fig. 4.3.5 shows the initial permeability for sintered ferrites using co-precipitation and mixed oxide methods at frequency ranging from 10 to 100 kHz. Results revealed that ferrites prepared from mixed oxide methods posses the higher initial permeability as compared to co-precipitation method.

According to Jeyadevan [60], MgCuZn ferrites of similar composition differ in their magnetic properties depending on the preparation technique. One of the reasons for such behavior is believed to be due to the differences in particle size. A decrease in particle size leads to an increase in non – magnetic fraction on the surface of the particle [79].

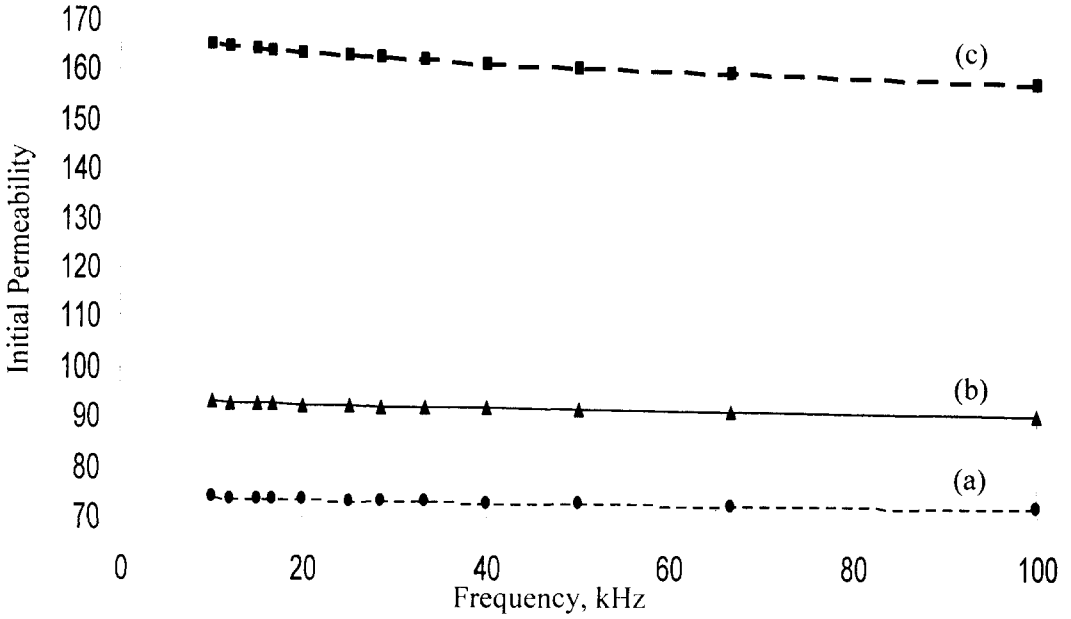

Fig. 4.3.5: Initial permeability measurement for specimens prepared by (a) co-precipitation process (CP 180-930), (b) co-precipitation and calcined (CP 650-930) and (c) mixed oxide route (MO 850-950)

According to particle size distribution analysis shows that the milled size of specimens prepared by co-precipitation process is smaller than those prepared by mixed oxide route. Furthermore, Specimens prepared by co-precipitation method consists of higher homogeneity during sample preparation as compared to those prepared by mixed oxide route. Specimens with smaller particle size and higher homogeneity should possess better magnetic behavior, but Fig. 4.3.5 shows differently. The lower initial permeability of co-precipitated specimens as compared to mixed oxide specimens might be due to the following reasons:

a. Small amount of impurity in starting materials might cause the deterioration in magnetic behavior of MgCuZn ferrites.

b. Small amount of sodium chloride left in MgCuZn ferrites might affect the magnetic properties.

c. Differences in magnetic properties of the specimens prepared by different methods might be also due to the differences in cation distribution, especially the distribution of the non–magnetic zinc ions, which will influence the magnetization.

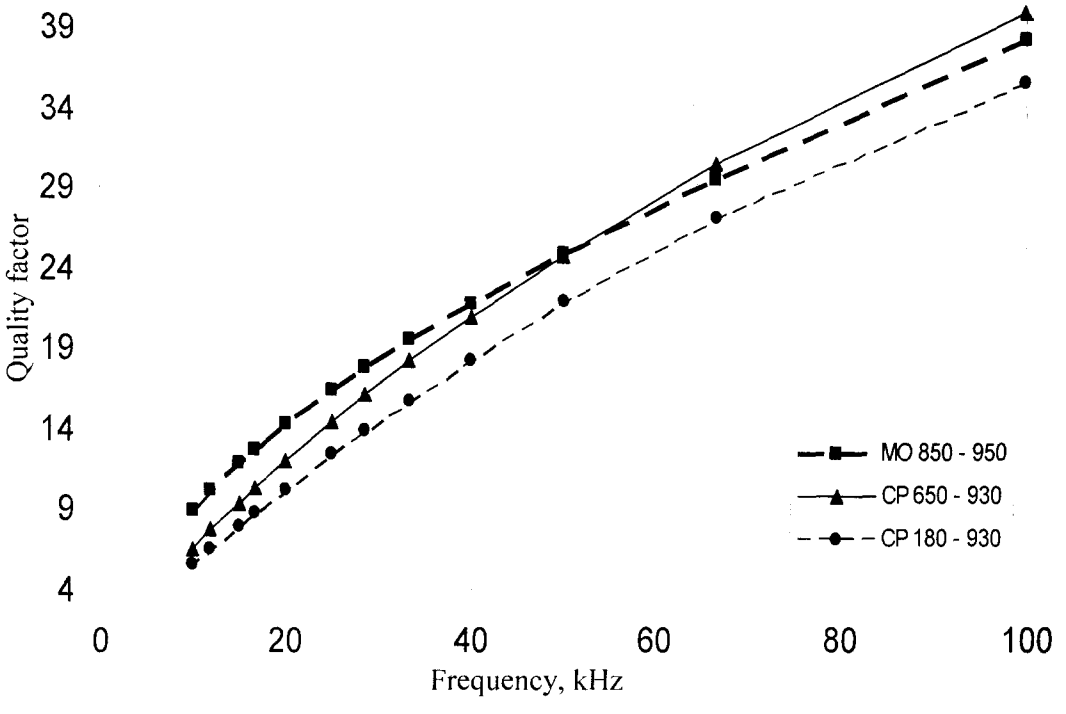

Fig. 4.3.6: Quality factor measurement for specimens prepared by co-precipitation process and mixed oxide route

Fig. 4.3.6 shows the quality factor for sintered ferrites using co-precipitation and mixed oxide methods at frequencies ranging from 10 to 100 kHz. The trend of the quality factor is different from the trend of the initial permeability.

Generally, throughout the frequency range from 10 to 100 kHz, the co-precipitated specimens dehydrated at 180°C and sintered at 930°C shows the lowest quality factor. However, others specimens has the highest quality factor depends on the frequency. Fig. 4.3.6 reveals that both specimens (CP 650 - 930 and MO 850 - 950) have the same quality factor value at about 50 kHz. Below the frequency of 50 kHz, the quality factor of the mixed oxide specimen (MO 850 – 950) is higher than the co–precipitated specimens (CP 650 – 930). However, above the frequency of 50 kHz, the quality factor of the mixed oxide specimen (MO 850 – 950) is lower than the co–precipitated specimen (CP 650 – 930).

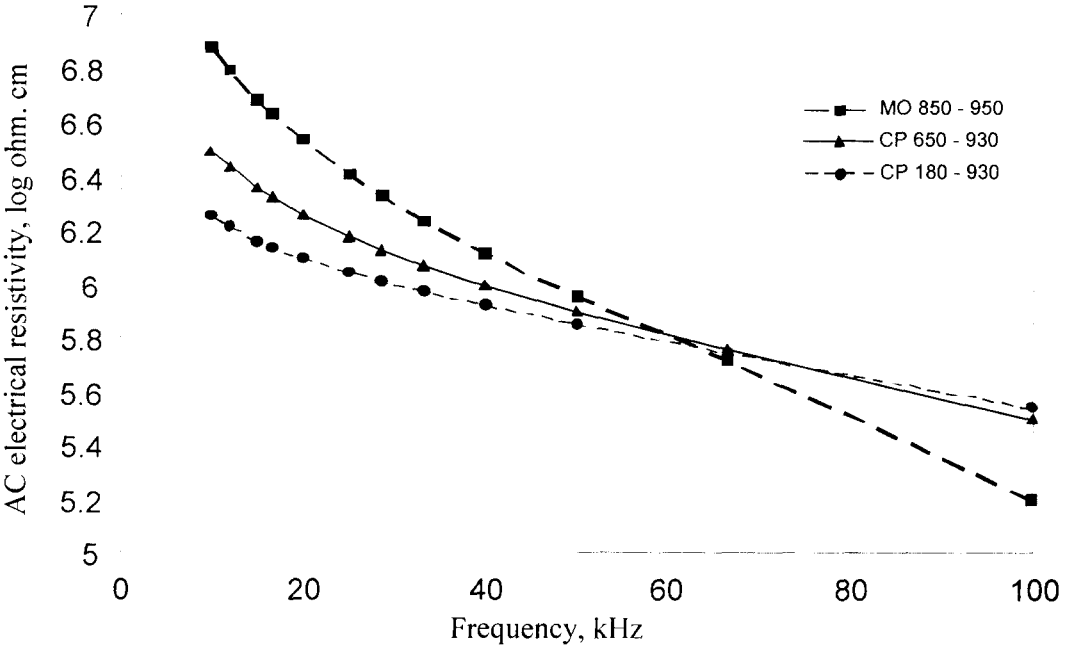

Fig. 4.3.7: AC electrical resistivity measurement for specimens prepared by co-precipitation process and mixed oxide route

Fig. 4.3.7 shows the AC electrical resistivity for sintered ferrites using co-precipitation and mixed oxide methods at frequencies ranging from 10 to 100 kHz. It reveals that all three specimens have the same AC electrical resistivity at frequency

about 60 kHz. Below the frequency of 60 kHz, the AC electrical resistivity of the mixed oxide specimen (MO 850 – 950) is higher than co – precipitated specimens. However, above the frequency of 60 kHz, the quality factor of the mixed oxide specimen (MO 850 – 950) is lower than co – precipitated specimens. Overall, throughout the frequency ranging from 10 to 100 kHz, the AC electrical resistivity of co – precipitated specimen (CP 650 – 930) is in between the AC electrical resistivity of mixed oxide specimen (MO 850 – 950) and co – precipitated specimen (CP 180 – 930).

The loss factor against frequency, ranging from 10 to 100 kHz, with different processing methods is shown in Fig. 4.3.8. It reveals that the specimens prepared by conventional method posses the lowest loss factor as compared to co - precipitation method.

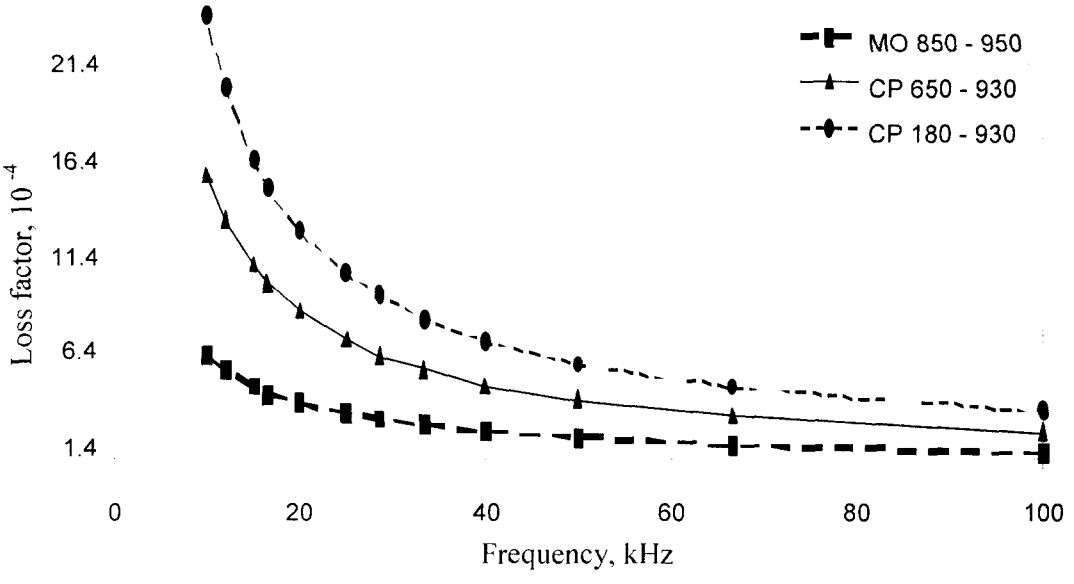

Fig. 4.3.8: Loss factor measurement for specimens prepared by co-precipitation process and mixed oxide route

MgCuZn ferrites were prepared by mixed oxide (conventional) and co-precipitation methods. Ferrites synthesized by conventional and co-precipitation methods achieve approximately the same range of densification, but have different electromagnetic properties. Ferrites prepared by conventional method show higher initial permeability and lower loss factor than ferrites prepared by the co-precipitation method. The lower initial permeability and higher loss factor of co-precipitated specimens as compared to mixed oxide specimens might be due to the following reasons:

a. Small amount of impurity in starting materials might cause the deterioration in magnetic behavior of MgCuZn ferrites.
b. Small amount of sodium chloride left in MgCuZn ferrites might affect the magnetic properties.
c. Differences in magnetic properties of the specimens prepared by different methods might be also due to the differences in cation distribution, especially the distribution of the non–magnetic zinc ions, which will influence the magnetization.

However, the trends of quality factor and AC electrical resistivity for conventional and co-precipitation method with frequency range are different.